

ON THE ORIGIN OF THE FUNDAMENTAL PLANE AND FABER-JACKSON RELATIONS: CONSEQUENCES  
FOR THE STAR FORMATION PROBLEM

MAURO D'ONOFRIO,<sup>1</sup> STEFANO CARIDDI,<sup>1</sup> CESARE CHIOSI,<sup>1</sup> EMANUELA CHIOSI,<sup>1</sup> AND PAOLA MARZIANI<sup>2</sup>

<sup>1</sup>*Department of Physics and Astronomy, University of Padova, Vicolo Osservatorio 3, I35122 Padova, Italy*

<sup>2</sup>*INAF - Padova Observatory, Vicolo Osservatorio 5, I35122 Padova, Italy*

(Received December 6, 2016)

Submitted to ApJ

ABSTRACT

The aim of this work is to show that the origin of the Fundamental Plane (FP) relation for early-type galaxies (ETGs) can be traced back to the existence of a fine-tuning between the average star formation rate  $\langle SFR \rangle$  of galaxies and their structural and dynamical characteristics. To get such result it is necessary to imagine the existence of two distinct "virtual planes" for each galaxy in the  $\log(R_e) - \log(\langle I_e \rangle) - \log(\sigma)$  space. The first one (named Virial Plane VP) represents the total galaxy mass using the scalar Virial Theorem and the mass-to-light ratio  $M/L$ , while the second plane comes from an expression of the total galaxy luminosity as a function of the mean star formation rate  $\langle SFR \rangle$  and the velocity dispersion  $\sigma$ , through a relation  $L = L'_0 \sigma^{-2}$  (named here pseudo-Faber-Jackson (PFJ)) which is a mathematical convenient way for expressing the independency of light from the virial equilibrium. Its validity can be connected to the mutual correlation  $L \sim \sigma \sqrt{\langle SFR \rangle}$  observed for all ETGs.

A posteriori it is possible to see that this approach permits to explain the observed properties of the FP (tilt and scatter) and the Zone of Exclusions (ZOE) visible in the FP projections. Furthermore, the link between the properties of the FP and the SFR of galaxies provides a new idea of the star formation, as a phenomenon driven by the initial conditions of proto-galaxies and regulated across the whole cosmic history by the variation of the main galaxy parameters (mass, luminosity, structural shape and velocity dispersion).

*Keywords:* Galaxies: early-types – Galaxies: structures and dynamics – Galaxies: Fundamental Plane  
– Galaxies: star formation

arXiv:1608.03502v3 [astro-ph.GA] 10 Dec 2016

## 1. INTRODUCTION

The origin of the Fundamental Plane, *i.e.* the relation:

$$a \log(R_e) + b \log(\langle I_e \rangle) + c \log(\sigma) + d = 0 \quad (1)$$

between the effective surface brightness, the effective radius and the central velocity dispersion of early-type galaxies (ETGs), is still unclear since the epoch of its discovery (Djorgovski & Davis 1987; Dressler et al. 1987). The problem consists in the observation that the FP coefficients deviate significantly from the virial expectation for homologous galaxies and in the fact that the scatter around the plane is very small along the whole FP extension.

The first interpretation of the tilt was related to the behaviour of the stellar populations of galaxies through their stellar mass-to-light ratio which was seen to vary with luminosity ( $M/L \sim M^\alpha$ , with  $\alpha \sim 0.25$  Faber et al. (1987)). Subsequent, independent measurements found similar values of  $\alpha$  (see *e.g.* Pahre et al. 1998; Gerhard et al. 2001; Borriello et al. 2001; Treu et al. 2005).

An alternative explanation was that galaxies are progressively non homologous systems along the FP (Hjorth & Madsen 1995; Prugniel & Simien 1997; Busarello et al. 1997; Graham & Colless 1997; Pahre et al. 1998; Bertin et al. 2002; Trujillo et al. 2004; Nipoti et al. 2006; La Barbera et al. 2010). This scenario was supported by the observation that the light profiles and dynamics of ETGs deviate systematically from homology (Capaccioli 1987; de Carvalho & da Costa 1988; Capaccioli 1989; Burkert 1993; Michard 1985; Schombert 1986; Caon et al. 1993; Young & Currie 1994; Prugniel & Simien 1997). Ciotti, Lanzoni & Renzini (1996) however pointed out that a strong fine-tuning between stellar mass-to-light ratio ( $M^*/L$ ) and structure (Sersic index  $n$ ) is required to explain with just structural non-homology both the tilt of the FP and the small scatter around it (the so-called  $M^*/L - n$  conspiracy). Cappellari et al. (2006, 2013) also excluded an important contribution of non-homology to the tilt using integral models of the ETGs mass distribution based on 2D kinematic maps. Along the same vein, the galaxy mass distribution estimated from gravitational lensing by Bolton et al. (2008) did not seem to support an important role for non-homology.

Subsequent interpretations of the tilt proposed a number of possible mechanisms: metallicity effects (Gerhard et al. 2001), dark matter distribution and amount (DM) (Tortora et al. 2009; Secco 2001; Secco & Bindoni 2009), dissipation effects during galaxy collapse (see *e.g.* Oñorbe et al. 2005; Dekel & Cox 2006; Robertson et al. 2006; Hopkins et al. 2008), variable initial mass function (IMF) (Chiosi et al. 1998), star formation history (SFH), etc., but the contribution of DM and IMF was also excluded by Ciotti, Lanzoni & Renzini (1996) on the basis of a required strong fine-tuning argument, and observing that the observed SFH of galaxies is hardly reconciled with the widely accepted hierarchical paradigm of the  $\Lambda$ CDM cosmology.

More recently D'Onofrio et al. (2013) proposed the existence of a fine-tuning mechanism able to explain the properties of the FP based on the observed mutual correlation between galaxy mass, mass-to-light ratio and Sérsic index.

In addition to the tilt the small observed scatter ( $\sim 20-25\%$ ) around the FP is also unexplained. Forbes et al. (1998) and Terlevich & Forbes (2002) found a correlation between the residuals of the FP and the age of the galaxies (ETGs with higher/lower surface brightness have younger/older ages). Gargiulo et al. (2009) claimed that the FP residuals anti-correlate with the mean stellar age, while a strong correlation exists with  $[\alpha/Fe]$ . Graves et al. (2009) proposed that the stellar population variations contribute at most 50% of the total thickness and that correlated variations in the IMF or in the central DM fraction make up the rest. Magoulas et al. (2012) found that the residuals about the FP show significant trends with environment, morphology and stellar population, with the strongest trend being with age.

The above discussion clearly reveals that a general consensus about the origin of the FP and its properties is still lacking. We remember that even the distribution of galaxies in the  $\log(\langle I_e \rangle) - \log(R_e)$  plane, *i.e.* one of the projections of the FP, is poorly understood. Kormendy (1977) showed that ETGs do not follow the distribution expected for galaxies of the same total luminosity, but are tilted with respect to this line, while Bender, Burstein & Faber (1992) and Burstein (1997) noted that in this plane galaxies seem to avoid a region of space: the so called Zone of Exclusion (ZOE). They claimed that the slope of the ZOE and the progressive displacement of the Hubble types from this line is consistent with the hierarchical clustering scenario with a  $n = 1.8$  power-law density fluctuation spectrum (plus dissipation).

The same considerations can be done for the Faber-Jackson relation connecting galaxy luminosity with velocity dispersion ( $L \propto \sigma^4$ ; Faber & Jackson 1976), whose slope (and zero point) changed progressively (today the measured slope is  $\sim 2.0$ ). This relation is considered a projection of the FP and as such was also related to the Virial Theorem, but alternative explanations are possible.

In this paper we propose a new possible solution for the origin of the FP and FJ relations able to explain all their observational properties. The paper is organized as follows: in the first section we present the main equations and assumptions that define the FP problem. In Sec. 3 we describe our proposed solution and in Sec. 4 we provide the observational evidences in favor of our hypothesis. In Sec. 5 we discuss the origin of the FJ and PFJ relations and in Sec. 6 the consequences of our solution for the problem of the star formation activity in galaxies across the cosmic history. Finally in Sec. 7 we draw our conclusions.

## 2. THE FP PROBLEM

We assume that ETGs are gravitationally bound stellar systems which satisfy the Virial Theorem equation:

$$\langle V^2 \rangle = \frac{GM_{tot}}{\langle R \rangle}. \quad (2)$$

where  $M_{tot}$  is the total galaxy mass,  $\langle R \rangle$  a suitable mean radius, and  $\langle V^2 \rangle$  a mean kinetic energy per unit mass. By definition every kind of virialized system must belong to the Virial Plane (VP) in the space defined by the variables  $M_{tot}$ ,  $\langle R \rangle$  and  $\langle V^2 \rangle$ . Unfortunately, these are not observable quantities. Therefore, in the case of ETGs, the Virial Eq. (2) is usually written as follows:

$$M_{tot} = \frac{K_V \sigma^2 R_e}{G} \quad (3)$$

where  $K_V = 1/(k_v k_r)$  takes into account projection effects, density distribution and stellar orbits distribution. The term  $K_V$  parameterizes our ignorance about the orientation, 3D structure and dynamics of ETGs. The formal expression of  $K_V$  (which is a dimensionless quantity) assumes:  $\langle V^2 \rangle = k_v \sigma^2$ , and  $\langle R \rangle = k_r R_e$ .

Introducing the mean effective surface brightness  $\langle I \rangle_e = L/2\pi R_e^2$ , one gets such expression for the Virial Plane (VP):

$$R_e = \frac{K_V}{2\pi G} \left( \frac{M_{tot}}{L} \right)^{-1} \langle I_e \rangle^{-1} \sigma^2, \quad (4)$$

or, in logarithmic form:

$$\begin{aligned} \log(R_e) = & 2 \log(\sigma) - \log(\langle I_e \rangle) + \log(K_V) + \\ & - \log\left(\frac{M_{tot}}{L}\right) - \log(2\pi G), \end{aligned} \quad (5)$$

This formulation of the Virial Theorem is directly comparable with the FP of Eq. (1) rewritten with  $\log(R_e)$  as independent variable as empirically derived from observations.

Note that for a given mass  $M_{tot}$  and zero point there are infinite values of  $\log(R_e) - \log(\langle I_e \rangle) - \log(\sigma)$  which satisfy Eq. (5): all the points belonging to a plane obey such equation. We can therefore define the VP as *the locus of points of the  $\log(R_e) - \log(\langle I_e \rangle) - \log(\sigma)$  space which reproduce a constant mass  $M_{tot}$  for an assigned zero point*. In other words the Virial Theorem does not provide any constraints on the position of a galaxy in the  $\log(R_e) - \log(\langle I_e \rangle) - \log(\sigma)$  space. Two galaxies with the same mass and zero point, but with a different combination of  $M/L$  and  $K_V$ , may share the same VP. In general Eq. (5) defines a family of planes filling the  $\log(R_e) - \log(\langle I_e \rangle) - \log(\sigma)$  space for all galaxies.

The zero point of Eq. (5) is given by the quantity:

$$ZP_{FP} = \log(K_V) - \log\left(\frac{M_{tot}}{L}\right) - \log(2\pi G), \quad (6)$$

so that each galaxy has its own zero point characterized by a peculiar  $M/L$  (dark matter and stellar content) and  $K_V$  (degree of non-homology). If ETGs were perfectly homologous systems (same  $K_V$ ) with similar  $M/L$  the  $ZP_{FP}$  would be a constant and all galaxies will be distributed along one VP.

In the  $\log(R_e) - \log(\langle I_e \rangle) - \log(\sigma)$  space each VP is parallel to the others, so that in principle one should observe a cloud and not a plane, unless some mechanism constrain all galaxies on the observed FP.

The connection between the FP and the VP clearly links the tilt of the plane to the properties of the stellar population, to the Dark Matter content and the galaxy structure and dynamics. It is therefore not surprising that all the proposed solutions have tried to demonstrate the link of the zero point with these galaxy properties. The existence of the FP, with its tilt and small scatter, requires a connection between  $K_V$  (structure) and  $M/L$  (DM and stellar populations). This is the so-called fine-tuning problem.

### 3. THE NEW PROPOSED SOLUTION

The new proposed solution comes from the observation that a galaxy of a given mass  $M_{tot}$  has not a defined position in the  $\log(R_e) - \log(\langle I_e \rangle) - \log(\sigma)$  space. Its virial equilibrium is guaranteed by all possible combinations of the variables that fit the virial equation. It would be nice to have at least another constraint to better define the location of a galaxy in the  $\log(R_e) - \log(\langle I_e \rangle) - \log(\sigma)$  space.

In order to find such constraint we consider that a galaxy of a given mass  $M_{tot}$  has also a total luminosity  $L_{tot}$ . The luminosity of a galaxy ultimately depends on the luminosities of its stars, that in turn depend on the star radius and the effective temperature that each star reaches at its surface.

The common way of introducing the luminosity in the FP problem was through the mass-to-light ratio, but we note that luminosity is actually a quantity independent on the virial equilibrium, being only the product of the SF history of galaxies.

On the basis of such consideration we look for the various expressions that can give the total luminosity of galaxies. We know that the integrated luminosity  $L$  of a galaxy of age  $T_G$  can be expressed as:

$$L = \int_0^\infty \int_0^{T_G} \int_{M_L}^{M_U} S(M, t, Z(t)) f_\lambda(M, \tau', Z(\tau')) dM dt d\lambda \quad (7)$$

where  $S(M, t, Z(t))$  is the stellar birth-rate,  $f_\lambda(M, \tau', Z(\tau'))$  is the monochromatic flux of a star of mass  $M$ , metallicity  $Z(t)$  and age  $\tau' = T_G - t$ , and  $M_L$  and  $M_U$  the minimum and maximum star masses that are formed. The stellar birth rate  $S(M, t, Z(t))$  can be expressed as the total mass converted into stars per unit time (e.g.  $M_\odot yr^{-1}$ ) or the total number of stars formed per unit time at the time  $t$  with the chemical composition  $Z(t)$ . We adopt the first definition for the sake of consistency with the definition of other quantities in usage here that are related to the star formation. Separating the  $S(M, t, Z(t))$  into the product of the SFR  $\Psi(t, Z(t))$  and the initial mass function  $\Phi(M, Z(t))$ , and neglecting here the dependence on the metallicity (it can be easily introduced whenever necessary) the above integral becomes

$$L = \int_0^\infty \int_0^{T_G} \Psi(t) F_\lambda(\tau') dt d\lambda \quad (8)$$

where

$$F_\lambda(\tau') = \int_{M_L}^{M_U} \Phi(M) f_\lambda(M, \tau') dM \quad (9)$$

where  $F_\lambda(M, \tau')$  is the integrated monochromatic flux at each epoch provided by a single stellar population of age  $\tau'$  and  $f_\lambda(M, \tau')$  is the monochromatic flux emitted by a star of mass  $M$  and age  $\tau'$  or  $t$  in general. Finally, we define the luminosity per unit mass of a single stellar population as

$$L_{sp}(t) = \int_0^\infty F_\lambda(t) d\lambda \quad (10)$$

and finally

$$L = \int_0^{T_G} \Psi(dt) L_{sp}(t) dt. \quad (11)$$

We can rewrite Eq. (11) considering the average values of the involved variables

$$L \sim \langle \Psi(t) \times L_{sp} \rangle T_G \quad (12)$$

where  $\langle \Psi(t) \times L_{sp} \rangle$  is the time averaged product of the current SFR and the luminosity of the stellar populations,  $T_G$  is the age of the galaxy. In the above average,  $L_{sp}$  indicates the mean stellar population representative of the whole stellar content. The emitted light is per unit mass. Eq. (12) is substantially telling us that the total luminosity of galaxies is the result of its SFH.

We also know however that the luminosity of ETGs is observed to correlate with the velocity dispersion of their stars through the Faber-Jackson relation (Faber & Jackson 1976).

$$L = L_0 \sigma^\beta \quad (13)$$

with  $\beta \sim 2 - 4$ . The origin of this correlation is obscure.

In the following we leave the expression in this form instead of scaling it in the form  $L = L_0(\sigma/\sigma_0)^\beta$  because we want to emphasize the physical meaning of the parameter  $L_0$  whose units are  $[gr/sec]$  consistent with a SFR if  $\beta = 2$ .

The fundamental question is why the galaxy dynamics should be aware of the stars that have been produced across the cosmic time.

Up to now the FJ relation has been considered a direct consequence of the Virial relation for systems where the mass-to-light ratio  $M/L$  vary systematically with the galaxy mass or luminosity. We will see below that alternative explanations are possible.

The direct comparison of Eq. (12) and Eq. (13) tells us that the parameter  $L_0$  of the FJ relation is connected to the mean SFR. We can in fact write:

$$L_0 = \langle \Psi(t) \times L_{sp} \rangle T_G / \sigma^2. \quad (14)$$

In this parameter is encrypted the complex relationship between the galaxy dynamics and the SFH.

#### 4. THE OBSERVED PROJECTIONS OF THE FUNDAMENTAL PLANE

What can we say observationally? Could we demonstrate the existence of a link between the Virial and FJ planes giving rise to the FP tilt? We will see here that this is not the case if  $\beta = 2$ .

From the observational point of view it is better to look at the projections of the FP, *i.e.* at the  $\log(\langle I_e \rangle) - \log(R_e)$  plane, the  $\log(\langle I_e \rangle) - \log(\sigma)$  plane and the  $\log(\sigma) - \log(R_e)$  plane.

The question is: where are located the projections of the intersecting lines, *i.e.* the lines of constant  $M/L$ ,  $K_V$  and  $L'_0$  in these 2D planes?

In order to answer such question we should consider Eqs. (1), (5) and to remember that  $L_{tot} = 2\pi \langle I_e \rangle R_e^2$ , so that passing to the logarithms Eq. 13 can be rewritten:

$$\begin{aligned} \log(R_e) &= (\beta/2) \log(\sigma) - (1/2) \log(\langle I_e \rangle) + \\ &+ (1/2) \log(L_0) - (1/2) \log(2\pi). \end{aligned} \quad (15)$$

The same equations can be also written as a function of  $\sigma$  in the following way:

$$\begin{aligned} \log(\sigma) &= A \log(R_e) + B \log(\langle I_e \rangle) + C \\ \log(\sigma) &= \frac{1}{2} \log(R_e) + \frac{1}{2} \log(\langle I_e \rangle) + \frac{1}{2} \log(M/L) + \\ &- \frac{1}{2} \log(K_V) + \frac{1}{2} \log(2\pi G) \\ \log(\sigma) &= \frac{2}{\beta} \log(R_e) + \frac{1}{\beta} \log(\langle I_e \rangle) + \\ &- \frac{1}{\beta} \log(L_0) + \frac{1}{\beta} \log(2\pi) \end{aligned} \quad (16)$$

where the coefficients  $A$ ,  $B$  and  $C$  are related to those of Eq. (1). Then we take the difference FP-VP and FP-FJ. These differences must be equal on the intersecting lines. It follows after some algebra that:

$$\log(\langle I_e \rangle) = \frac{(2/\beta) - (1/2)}{(1/2) - (1/\beta)} \log(R_e) + \Pi \quad (17)$$

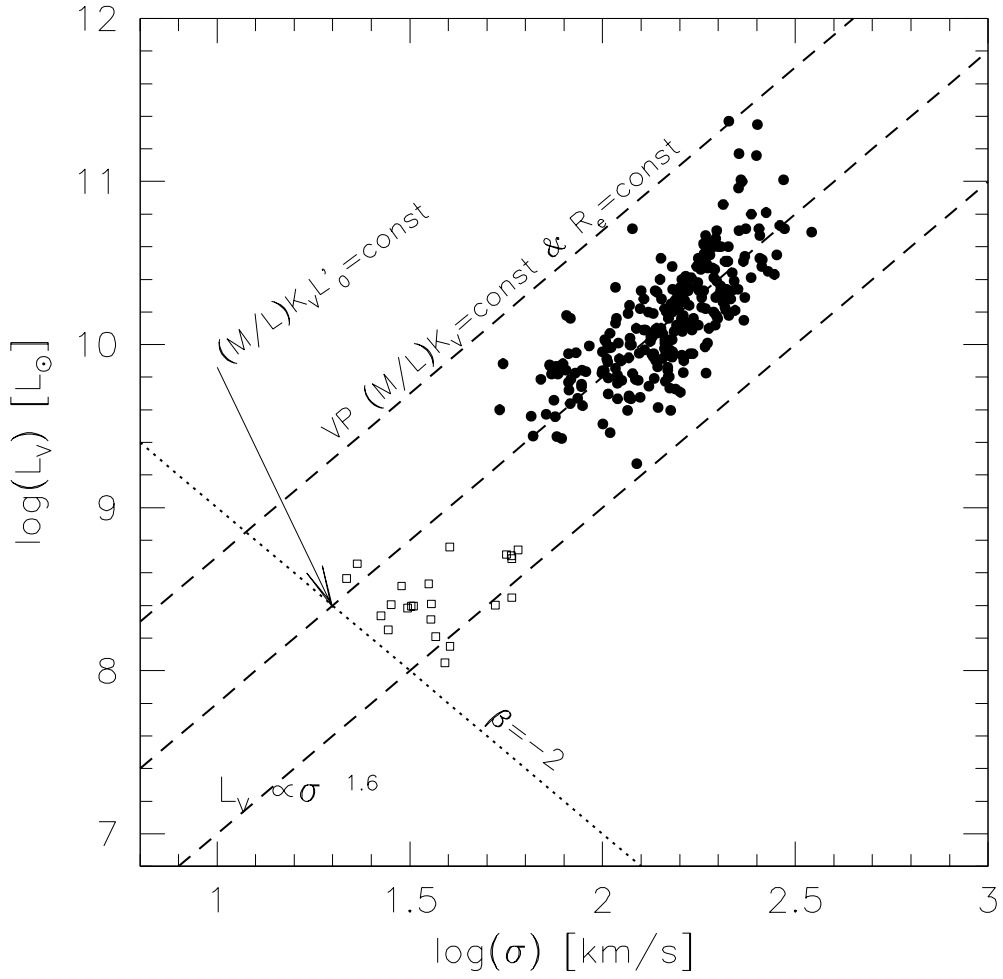


**Figure 1.** The  $L - \sigma$  plane. The fitted FJ relation for the ETGs of the WINGS database (Moretti et al. 2014) is given by the solid line. The dashed lines mark the position of the VPs for galaxies with different effective radii and zero-point. The dotted line marks one possible PFJ plane with  $L'_0 = \text{constant}$  with slope equal to  $-2$  (see text). The classical FJ relation seems to result from the intersection of the PFJ and the VP planes. The filled circles are normal ETGs. The open squares are dwarf galaxies of the WINGS database with masses around  $10^8 - 10^9 M_\odot$ .

where  $\Pi$  contains all terms not explicitly written in the Eq. (17).

Now we ask ourselves if Eq. (13) could represent the plane we are looking for in the  $\log(R_e) - \log(\langle I_e \rangle) - \log(\sigma)$ . First we observe that in the FJ relation  $L_0$  is nearly constant for almost all ETGs (in the mass range  $10^9 - 10^{12} M_\odot$ ) of different  $\sigma$ . So this relation is not the one we are looking for as a second virtual plane representing the total luminosity of a galaxy in the  $\log(R_e) - \log(\langle I_e \rangle) - \log(\sigma)$  space. Furthermore for  $\beta = 2$  Eq. (17) the slope of the  $I_e - R_e$  relation is undefined.

Looking at Fig. 1 we note instead that an alternative way of writing  $L_{tot}$  is possible and mathematically correct:

$$L = L'_0 \sigma^\beta \quad (18)$$

where the value of  $\beta$  could be chosen on the basis of the observed distribution of galaxies in the FP projections. We will see that the best value for  $\beta$  is  $-2$ . The slope of such relation is marked by the dotted line in Fig. 1.

With such a relation we assign to  $L'_0$ , which is very different from galaxy to galaxy, the primary role of capturing the SFH of each object leaving to  $\sigma$  the secondary role of indicating how the velocity dispersion affects the SFR ( $\sigma$  could only change in a limited interval, that provided by the scatter of the FJ relation).

Being  $L'_0$  and  $L_0$  correlated we have that  $L_0 = L'_0 \sigma^{-4}$ . It follows on the basis of Eq.(12) that also  $L'_0$  is connected to the SFR:

$$L'_0 = \langle \Psi(t) L_{sp} \rangle T_G \sigma^2. \quad (19)$$

Now substituting  $L'_0$  to  $L_0$  in Eq. 15 we obtain a plane in the  $\log(R_e) - \log(\langle I_e \rangle) - \log(\sigma)$  space which is tilted in the right direction with respect to the VP and with the notable property of having a significantly different zero-point for each galaxy.

This is the second virtual plane of the  $\log(R_e) - \log(\langle I_e \rangle) - \log(\sigma)$  that we are looking for. It represents the total luminosity of a galaxy with a zero-point different for each object as it is the case for the total mass in the VP (through  $(M/L)$  and  $K_V$  as zero-points).

We call this plane the "PFJ plane" (pseudo-FJ) for keeping in mind its origin from the FJ relation and we define it as follows: *The PFJ plane is the locus of points defined by the values of  $\log(R_e) - \log(\langle I_e \rangle) - \log(\sigma)$ , which reproduce a constant luminosity  $L_{tot}$  for an assigned zero point  $L'_0$ .* This plane contains, as the VP, only one galaxy and all PFJ planes are parallel each other in the  $\log(R_e) - \log(\langle I_e \rangle) - \log(\sigma)$  space.

The different inclination of the VP and PFJ planes suggests that they intersect somewhere in the  $\log(R_e) - \log(\langle I_e \rangle) - \log(\sigma)$  space, forming a line in such space. Along this line it resides only one object, that with mass  $M_{tot}$ , luminosity  $L_{tot}$  and zero points  $Z_{FP}$  and  $Z_{PFJ} = 1/2 \log(L'_0)$ . In other words along this line, the product  $(M/L)K_V L'_0$  is constant.

It is clear that if the zero points of the VP and PFJ planes vary in a coordinated way, the result will be that of forming several parallel lines in the  $\log(R_e) - \log(\langle I_e \rangle) - \log(\sigma)$  space, each one containing one galaxy. The plane best fitting this distribution of parallel lines is the plane of real galaxies in the  $\log(R_e) - \log(\langle I_e \rangle) - \log(\sigma)$  space, *i.e.* the FP. We therefore define the FP as follows: *The FP is the plane in the  $\log(R_e) - \log(\langle I_e \rangle) - \log(\sigma)$  space that best fit all the parallel lines formed by the intersections of the VP and PFJ planes. In this plane the quantity  $(M/L)K_V L'_0$  is constant.* In this framework, the existence of a FP for real galaxies implies that a close connection must exist between  $(M/L)$ ,  $K_V$  and  $L'_0$  (or in other words between mass, luminosity, structure and SFR).

A graphical representation of the mechanism originating the FP is given in Fig.2. The upper panel of the figure shows two VPs for two galaxies (in black and gray) and one PFJ plane for one galaxy. The intersecting line formed in the  $\log(R_e) - \log(\langle I_e \rangle) - \log(\sigma)$  by the two planes for a galaxy of mass  $M_{tot}$  and luminosity  $L_{tot}$  marks the locus in which galaxy might reside.

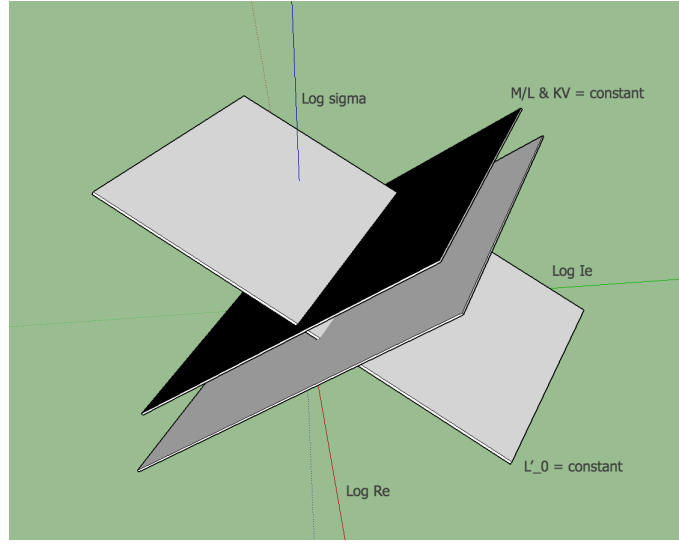
Consequently, the FP plane is naturally tilted with respect to both the VP and PFJ planes. Its tilt is now connected to the global variation of the zero points of the VP and PFJ planes ( $Z_{FP}$  and  $Z_{PFJ}$ ), and the small scatter observed around the plane originate from the fine-tuning effect linking  $M/L$ ,  $K_V$  and  $L'_0$ , *i.e.* linking the galaxy mass, structure and dynamics with the SFR of galaxies. In view of the future use it is mathematically convenient to assume:

$$\begin{aligned} \Pi = \frac{1}{2} \log(K') = & \frac{[\frac{1}{2} \log(K_V) - \frac{1}{2} \log(M/L)]}{[\frac{1}{2} - \frac{1}{\beta}]} + \\ & + \frac{[-\frac{1}{\beta} \log(L'_0) - \frac{1}{2} \log(2\pi G) + \frac{1}{\beta} \log(2\pi)]}{[\frac{1}{2} - \frac{1}{\beta}]} \end{aligned} \quad (20)$$

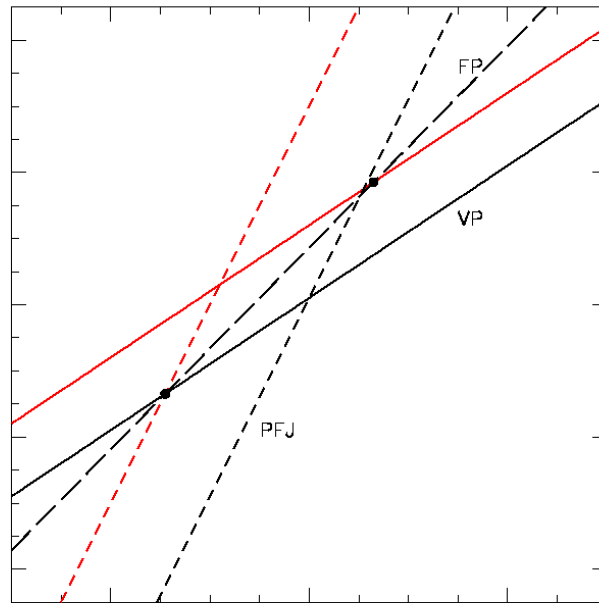
which also defines the constant  $K'$ .

We have obtained an equation for the distribution of galaxies with similar  $M/L$ ,  $K_V$  and  $L'_0$  in the  $\log(\langle I_e \rangle) - \log(R_e)$  relation. The zero point of Eq. (17) varies as  $M/L$ ,  $K_V$  and  $L'_0$  vary in the FP space. Note that the slope of the relation depends only on the value of  $\beta$ , *i.e.* on the exponent of the PFJ plane.

Fig.3 shows the  $\log(\langle I_e \rangle) - \log(R_e)$  plane where we have adopted the solution of Eq. (20) with  $\beta = -2$ . Note how this value of  $\beta$  naturally reproduces the slope of the observed distribution of galaxies. It follows that the so called ZOE (Zone of Exclusion) is in this context a natural limit reached today by the values of  $M/L$ ,  $K_V$  and  $L'_0$  during the cosmic evolution.



(a)



(b)

**Figure 2.** Panel (a): General view of the  $\log(R_e) - \log(\langle I_e \rangle) - \log(\sigma)$  with two VPs and one FPJ plane. Panel (b): Two possible VP and FPJ planes seen edge-on for two ETGs of masses  $M_1$  and  $M_2$  and luminosities  $L_1$  and  $L_2$  respectively are shown with black (VP) and red lines (FPJ). The FP results in this case from the connection of the two intersections of the VP and PFJ planes. For many galaxies the FP is the plane best fitting all the intersecting lines.

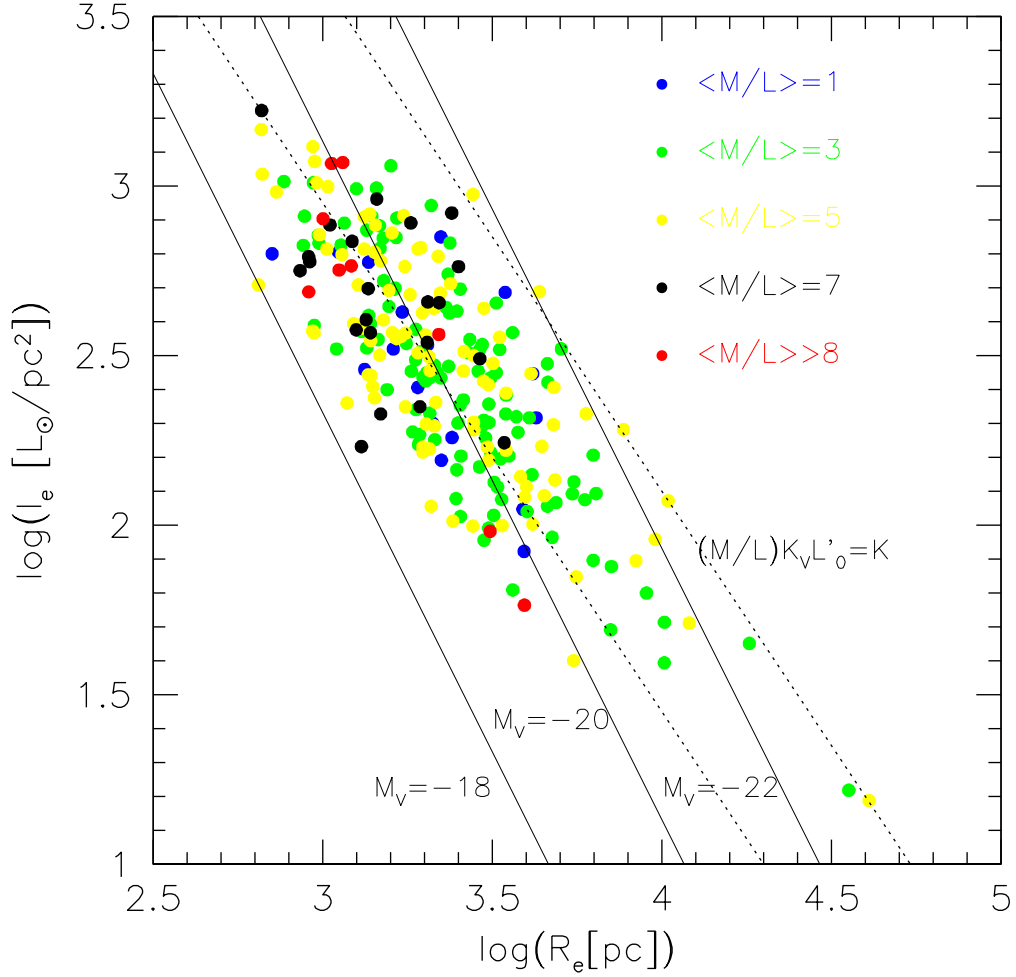


**Figure 3.** The  $\log(\langle I_e \rangle) - \log(R_e)$  plane of the WINGS ETGs. Galaxies are plotted with different colors according to their measured stellar  $M^*/L$  as indicated. The solid lines give the locus of constant galaxy luminosity. The dotted lines mark the locus of constant  $M/L$ ,  $K_V$  and  $L'_0$ , *i.e.* the projections of the intersecting lines originating the FP.

In the figure we plotted with different colors different ranges for the stellar  $M^*/L$  ratios available for the galaxies of the WINGS database in the V-band (Moretti et al. 2014). Note that there is not a clear trend in the  $M^*/L$  ratios, even if the higher mass-to-light ratios seem more frequently distributed far from the ZOE.

Fig.4 is instead a plot of the  $\log(\langle I_e \rangle) - \log(R_e)$  distribution for objects of very different masses, covering a range from  $\sim 1M_\odot$  to  $\sim 10^{14}M_\odot$ , *i.e.* from stars to clusters of galaxies. The data for the GC systems are taken from Pasquato & Bertin (2008), those for stars are taken from Wikipedia and that for dwarf galaxies and galaxy clusters come from the WINGS database (Cariddi et al. in prep.).

Note that the  $\log(\langle I_e \rangle) - \log(R_e)$  relation seems to be valid on all scales. For stars the  $M^*/L$  ratio increases as far as we move away from the ZOE going from the main sequence stars of A spectral type to that of M type stars. If the dominating stellar population inside a stellar system is made of late type stars we will observe an higher ( $M^*/L$ ) that will likely place the galaxy far from the ZOE<sup>1</sup>.

<sup>1</sup> Assuming that the DM contribution is approximately the same for all galaxies, which is not exactly the case.

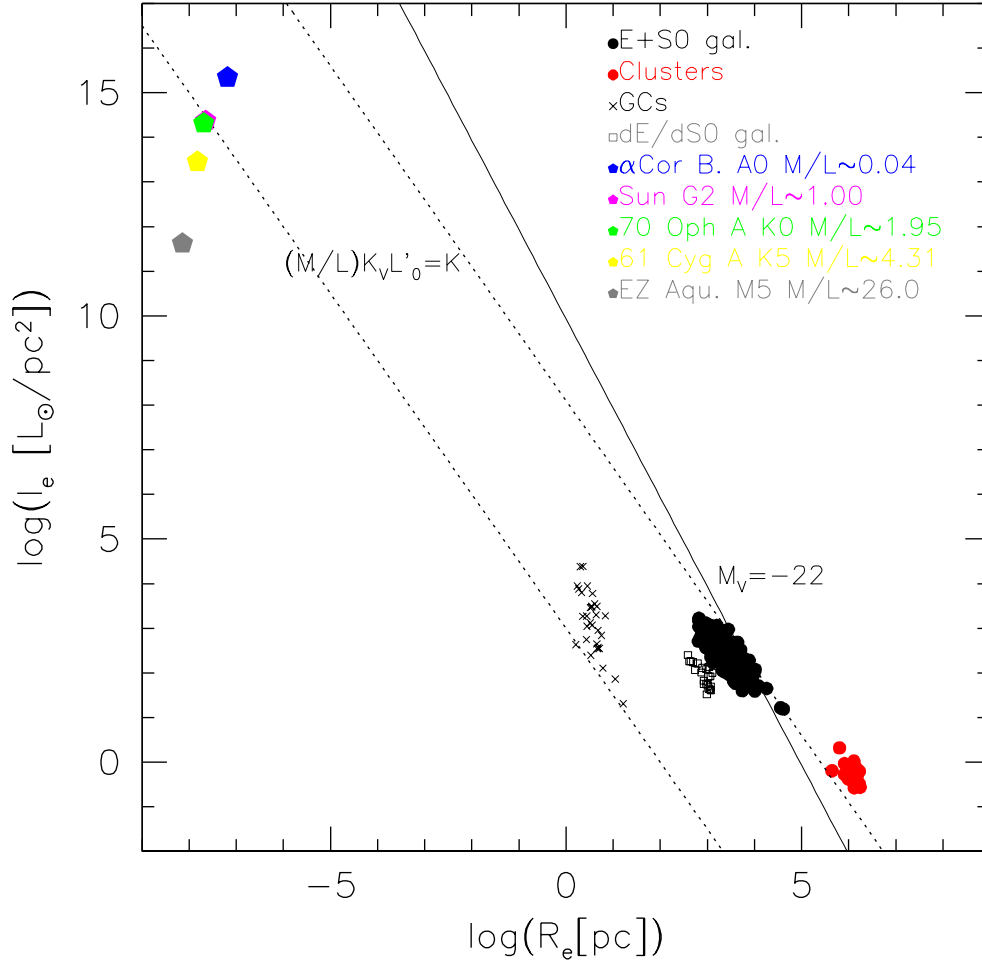


**Figure 4.** The  $\log(\langle I_e \rangle) - \log(R_e)$  plane for objects of different masses that are known to be close to the virial equilibrium: main sequence stars, globular clusters, dwarf galaxies, normal ETGs and galaxy clusters. The solid lines give the locus of constant absolute magnitude, while the dotted lines are parallel to the ZOE. The lower dotted line marks the position of  $M/L = 1$  ( $M_\odot/L_\odot$ ).

Note also that this diagram is done for the V-band, so that there is a natural selection effect working on, since the lower ( $M^*/L$ ) due to bright stars that dominate the galaxy luminosity, progressively move the galaxies toward the ZOE.

The galaxy clusters appear shifted with respect to the ZOE because these systems contain several spiral galaxies with low  $M^*/L$ , while Globular Clusters have a solar mass-to-light ratio because their stellar population is dominated by stars with high ( $M^*/L$ ).

For the other FP projections we obtain:

$$\begin{aligned} \log(\langle I_e \rangle) &= (\beta - 1) \log(\sigma) + const \\ \log(\sigma) &= \frac{1}{2 - \beta} \log(R_e) + const, \end{aligned} \quad (21)$$

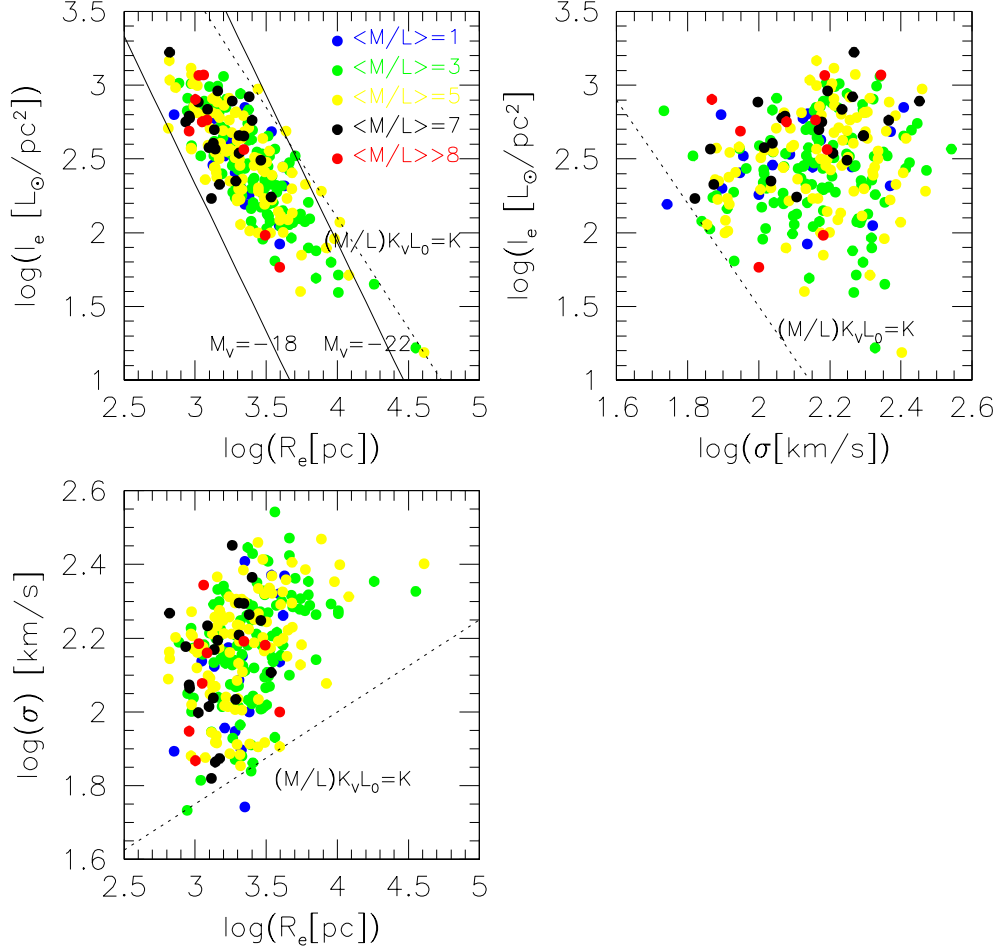


**Figure 5.** The different projections of the FP on the  $\log(R_e) - \log(\langle I_e \rangle) - \log(\sigma)$  axes. The dotted lines mark a possible position for the ZOE.

where the constant zero points also depend on the combination of  $M/L$ ,  $K_V$  and  $L'_0$ . Again the  $\beta = -2$  value determines the distribution of galaxies and the position of the ZOE in the respective diagrams (see Fig.5).

In conclusion, we have obtained the FP by fitting in the  $\log(R_e) - \log(\langle I_e \rangle) - \log(\sigma)$  space the distribution of the parallel lines where for each galaxy two virtual planes intersect each other. The first plane is provided by the Virial Theorem and fixes the mass of a galaxy once the  $M/L$  and  $K_V$  zero point are given. The other comes from having written the total galaxy luminosity with the  $L = L'_0 \sigma^{-2}$  relation, encrypting in the parameter  $L'_0$  the role played by the SF activity.

In the next section we will further discuss the possible origin of the connection between luminosity and velocity dispersion in ETGs and the nature of the  $L_0$  and  $L'_0$  parameters.

## 5. MORE ON THE FJ AND PFJ PLANES

Why  $L$  and  $\sigma$  are correlated variables? A priori there are no reason at all for such a connection. A posteriori we understand it on the basis of the connection between mass and luminosity in each single star and on the basis of the virial theorem. The SF is a local phenomenon originating by micro-physical processes inside clouds of gas and dust,

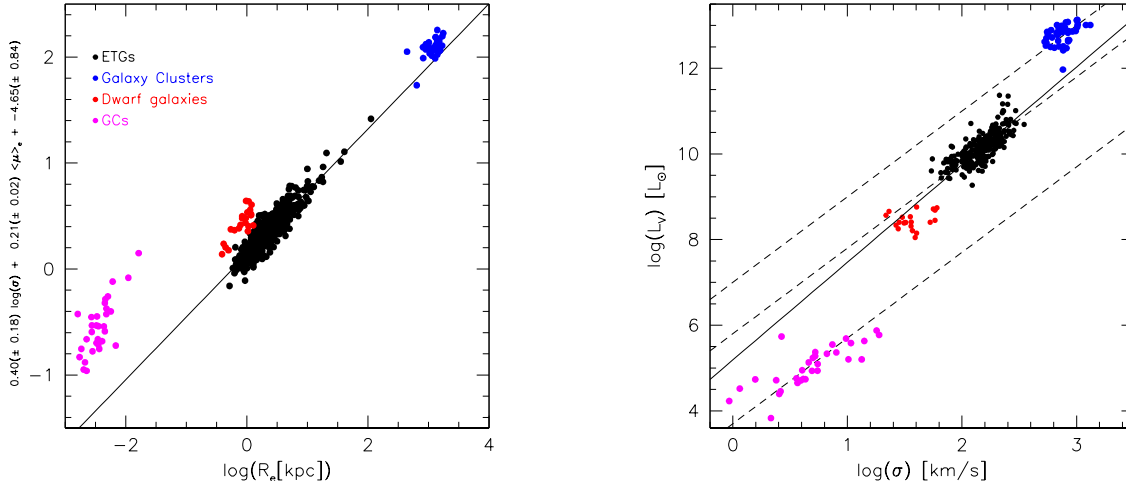


**Figure 6.** Top: an edge-on view of the FP for all types of stellar systems. Bottom: the same systems on the FJ relation.

while the velocity dispersion is a direct consequence of the mass potential well. How the two things communicate? This is a classic example of a recurrent problem in physics concerning the connection between microscopic and macroscopic phenomena.

Before attempting any possible answer we want to better describe here the  $L - \sigma$  plane, which is actually very different from the VP. The FJ plane contains two measured quantities, the galaxy luminosity and the stellar velocity dispersion. At variance with the VP that is defined for one galaxy only in the  $\log(R_e) - \log(\langle I_e \rangle) - \log(\sigma)$  assigning its mass and zero point, the FJ plane contains all real galaxies at the same time. Along the fitted relation the zero point  $L_0$  is nearly constant for almost all galaxies (let say between  $10^9$  and  $10^{12} M_\odot$ ).

The first thing to note is that in the FJ plane the points of constant  $M/L$ ,  $K_V$  and  $L'_0$  are the galaxies themselves (see again Fig.1). Note how the selected solution with  $\beta = -2$  used for the  $\log(\langle I_e \rangle) - \log(R_e)$  relation gives here the series of parallel zero points that for each  $\sigma$  provides the luminosities of all galaxies reproducing the observed FJ relation when they are considered all together. The FJ relation seems to originate from the intersections of the "projections" in the  $L - \sigma$  space (having collapsed  $I_e$  and  $R_e$  in the variable  $L$ ) of all the parallel virtual planes that represent the total luminosity of galaxies with the "projections" arising from the virial planes (the dashed lines where  $M/L$ ,  $K_V$  and  $R_e$  are constants). The intersection of the  $L = L'_0 \sigma^{-2}$  line with the VP projection fixes the exact position of a galaxy in the  $L - \sigma$  space.

The result is the relation expected for all virialized stellar systems having similar zero-point  $L_0$ . In this context it is therefore possible to explain why the residuals from the FJ relation correlate with the  $(M/L)$  ratio (Cappellari et al. 2006) and with galaxy sizes (Desmond & Wechsler 2016).

Note also that dwarf galaxies ( $M \sim 10^{8 \div 9} M_\odot$ ) deviate from the main galaxy relation. This occurs for the same reason why these stellar systems deviate from the FP (see Fig.6): they have a zero point systematically different, *i.e.* different  $M/L$ ,  $K_V$  and  $L'_0$  values. The upper and lower panels of this figure clearly show that all stellar system seem to obey to the FP and FJ relations, but with zero points slightly different from that of typical galaxies. These variations are responsible of the larger exponent observed in many cases for the FJ relation (4 instead of 2), which ultimately depends on the heterogeneity of the galaxy sample, *i.e.* from the inclusion of galaxies of very different masses and zero-points. An extreme example is seen in the right panel of Fig.6, where a steeper slope for the FJ can be obtained with a fit for objects of very different masses (and zero-points).

However, the FJ law is a relation that provides a further element to the virial relation, linking mass (and the virialized system internal gravitational energy) to the production of radiant energy *i.e.*, to the object luminosity. The mechanisms of production of energy can be very different and can yield to widely different  $M/L$  even among stellar systems, where the mechanism is roughly the same, ultimately associated with nuclear reactions in the star interior.

If we now take Eq. (20) with  $\beta = -2$ , giving the zero point of the relationship between the effective surface brightness  $I_e$  and the effective radius  $R_e$  (the zero point varies with  $M/L$ ,  $K_V$  and  $L'_0$  and hence with  $Z_{FP}$ ), after few steps we get:

$$K' = \frac{K_V}{4\pi^2 G} \frac{L}{M} L'_0 \quad (22)$$

where  $L'_0$  is  $L/\sigma^{-2}$  and  $K'$  is a parameter different for each cosmic epoch with units of  $[gr^2 cm^3 sec^{-6}]$  (or  $[L_\odot^2/pc]$ ), the gravitational constant is given in cgs units or expressed as  $G = 4.3 \times 10^{-3} pc M_\odot^{-1} (km/s)^2$  and the term  $K_V$  is a function of the Sersic index  $n$  (see, Bertin et al. 2002).  $K'$  will follow the evolution of the main galaxy parameters by changing the position of a galaxy in the  $\log(\langle I_e \rangle) - \log(R_e)$  plane. As a consequence the whole FP is expected to vary its tilt across the cosmic epochs.

The quantity  $L'_0$  is the zero-point of the  $L = L'_0 \sigma^{-2}$  relation. It is marked by the dotted line in Fig. 1 in the FJ space, and intersects the VP lines originating the observed FJ law. Fig.7 shows the relation between  $L'_0$  derived from Eq. (22) and the total galaxy luminosity  $L$ . Here we used the stellar  $M^*/L$  being  $M/L$  unknown. We observe that the link of  $L'_0$  and  $L$  is far from being trivial ( $L'_0$  results from a complex combination of  $M/L$  and  $K_V$ ), and the same could be said for the dependence of the residuals to the central velocity dispersion  $\sigma$ .

Fig. 8 gives a clear indication that both  $L$  and  $L'_0$  are correlated with the mean SFR of the galaxies measured by Fritz et al. (2007). The residuals present a significant dependence on  $\sigma$ . All these things tell us that we should look at the correlation of the three variables  $L$ ,  $\sigma$  and  $\langle SFR \rangle$ . These are mutually connected because the mass  $M$  correlate with the velocity dispersion  $\sigma$  through the virial relation and the light  $L$  correlate with the mean star formation rate  $\langle SFR \rangle$ . Consequently  $\sigma$  and  $\langle SFR \rangle$  are connected. Fig. 9 provides two angle views of the 3D distribution of such variables. Note the elongated sigar-shape distribution of ETGs in this space.

The 3D correlation between these variables gives:

$$\log(L) = 0.48(\pm 0.06) \log(\langle SFR \rangle) + 1.00(\pm 0.13) \log(\sigma) \quad (23)$$

with an  $rms = 0.215$  ( $R = 0.64$  and  $p - value < 1.2 \times 10^{-16}$ ). Therefore  $L \sim \sigma \sqrt{\langle SFR \rangle}$ . It is clear in this context that the  $L = L'_0 \sigma^{-2}$  relation represents the most convenient way of assigning a role to the SFR of each galaxy in the  $L - \sigma$  plane.

We want also to note that the quantity  $L'_0$  gives the opportunity of quantify the DM content of ETGs. Fig. 10 shows the comparison of the values of  $\log(L'_0)$  derived from Eq. 22 and from the relation  $L = L'_0 \sigma^{-2}$ . Since along the y-axis we have only the observed stellar  $M^*/L$  ratio while along the x-axis a quantity depending on the total galaxy mass, it is possible to see that going toward more massive systems a progressively larger fraction of DM is required to get the equivalence between the two quantities<sup>2</sup>.

The nature of the  $L_0$  and  $L'_0$  parameters remains however quite elusive. Behind them is encrypted the complex interconnection between the SF process and the galaxy dynamics.

We note that Eqs. (22) and (A13) give consistently for  $L_0$  a mean value of  $1.6 \pm 2.8 \times 10^{29} [gr/sec]$ . Where this value come from? We explored if the observed value of  $L_0$  could be linked to the amount of matter burned by nuclear reactions inside stars in each second. Considering in fact only the H-burning of main sequence stars, we know that  $\sim 10^{18 \div 19} [erg]$  comes from the nuclear burning of 1  $gr$  of Hydrogen, so that at least  $\sim 10^{26 \div 27} [gr]$  are burned each second in a galaxy with  $10^{12}$  stars similar to the Sun. The remaining contribution can be easily explained taking into account that the light from a galaxy comes prevalently from RGB stars  $\sim 1000$  more luminous than the Sun which are burning Hydrogen in shells. This however rises the problem of explaining why  $L_0$  is the same for galaxies of different masses (from  $10^9$  to  $10^{12}$  solar masses). Eq. (14) offers a more credible explanation for this: big/small systems have a larger/lower mean SFR and also a larger/lower velocity dispersion in such a way that the two compensate each other providing similar values of  $L_0$  for many galaxies. We will see in Appendix how it is possible to achieve the observed values of  $L_0$  by looking at the FJ relation along a different perspective.

$L'_0$  on the other hand is peculiar for each galaxy and in some way can be considered a proxy of the so-called downsizing phenomenon, remembering the very different SFH of each galaxy.

In summary we can say that we have two different independent correlations. The first one is that between mass  $M$  and velocity dispersion  $\sigma$  provided by the virial theorem. The second one is that between luminosity  $L$  and mean SFR

<sup>2</sup> Here the gas contribution to the total mass of the system is not taken into account

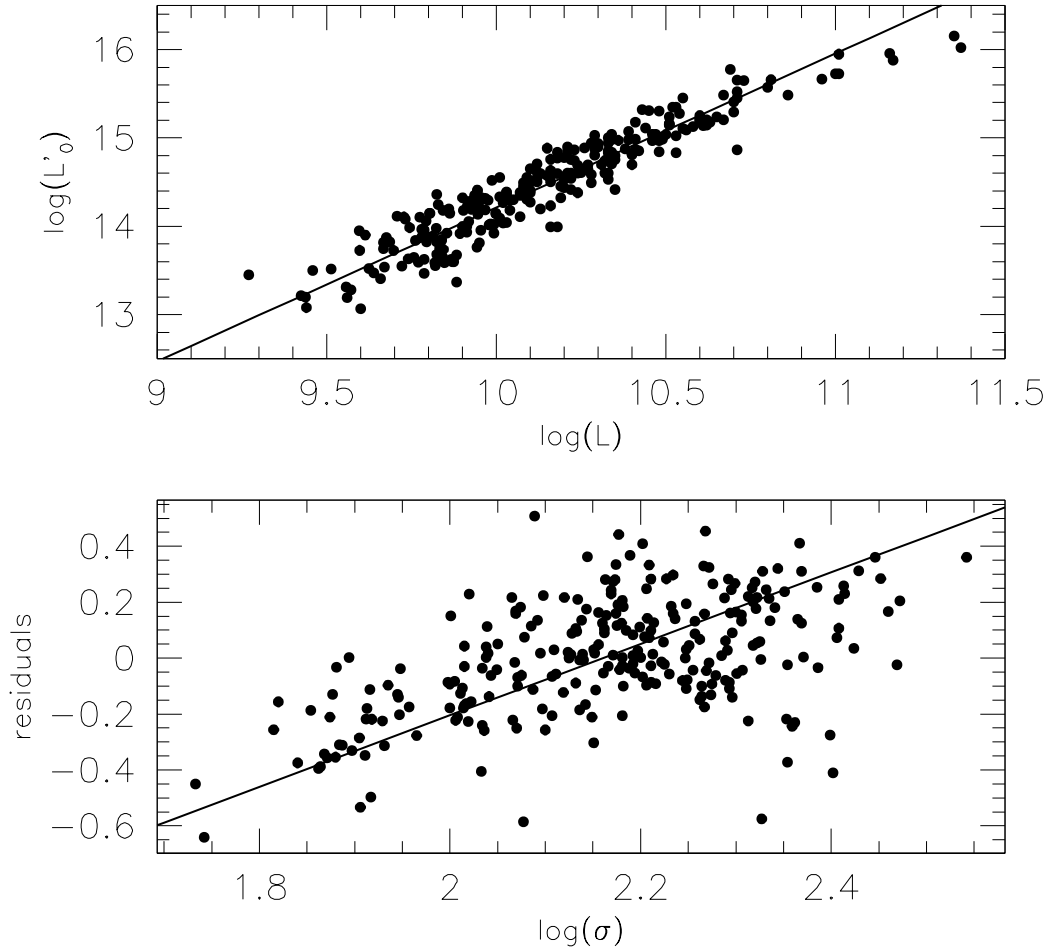


**Figure 7.** Upper panel: Plot of  $L'_0$  derived from Eq. 22 vs the measured total galaxy luminosity  $L$ . Lower panel: Plot of the residuals from the best fit of the above relation versus the measured velocity dispersion  $\sigma$ .

$\langle SFR \rangle$ . Once we substitute  $M$  with  $L$  in the virial relation we get the FJ relation, where  $L_0 = R_e L / GM$  (that is equal to  $\sim 1.6 \times 10^{29} \text{ gr/s}$ ). With such substitution when we look at the 3D space provided by  $L - \sigma - \langle SFR \rangle$  (in log units) we observe a sigar-shape distribution and we create a link between  $\sigma$  and  $\langle SFR \rangle$  that are indirectly correlated.

With this in mind we now understand why we should use the  $L = L'_0 \sigma^{-2}$  relation for building the second virtual plane in the  $\log(R_e) - \log(\langle I_e \rangle) - \log(\sigma)$  space. In fact in order to build such plane we need to use the direct correlation between  $L$  and  $\langle SFR \rangle$  valid for each galaxy and not the one between  $L$  and  $\sigma$  valid for all galaxies. This because we want to express the galaxy luminosity in a way independent on its mass. The  $L - \langle SFR \rangle$  relation has  $\sigma$  as second hidden parameter as we have seen.

In the next section we will further explore the consequences of our findings for the problem of the star formation activity in galaxies.

## 6. THE SF ACTIVITY IN GALAXIES

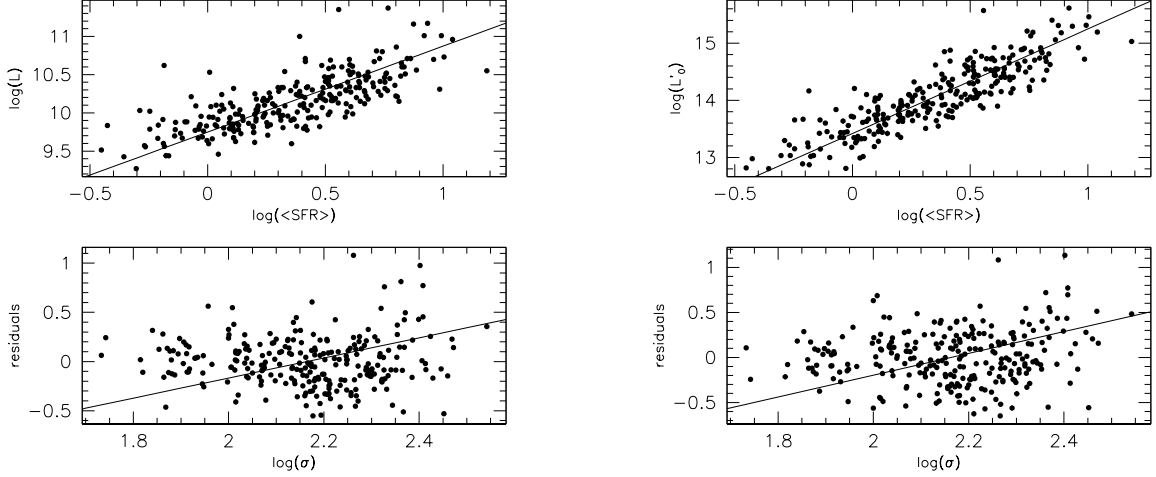


**Figure 8.** Plot of  $L$  and  $L_0$  vs the mean SFR in log units. Note that the residuals of these relations depend on  $\sigma$ .

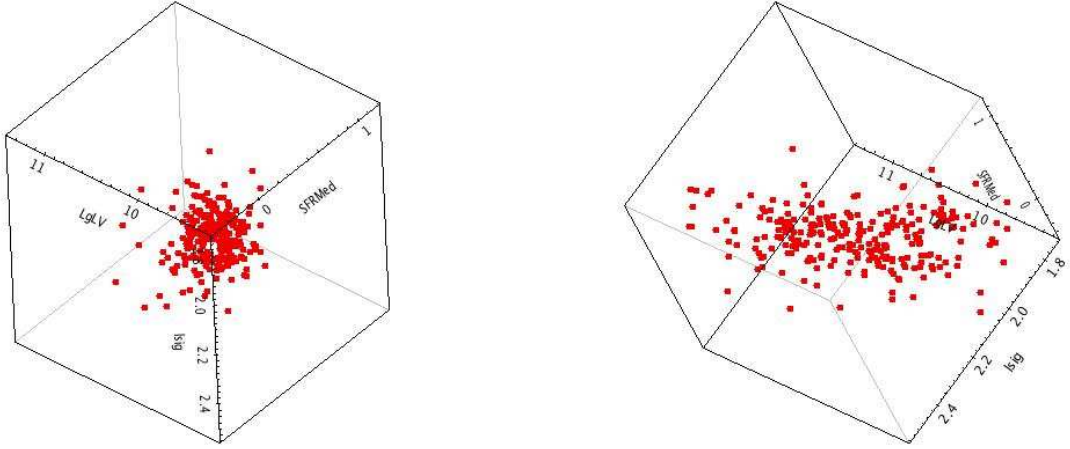


**Figure 9.** Two 3D views of the correlation between  $L$ ,  $\langle SFR \rangle$  and  $\sigma$  in log units.

Eq. (14) provides a link between  $L_0$  and the mean SFR of galaxies. It does not give a direct link between the current SFR, the velocity dispersion and  $L_0$ .

What we are looking for is a more direct link between these quantities. How are they connected? We will show in Appendix that the FJ relation can be interpreted as a possible translation of the Stefan-Boltzmann' law valid for stars to the case of stellar system, putting in evidence that it is always possible to express the energy of a system with the more convenient units (the ones we can measure).

Doing this exercise we have noted that the galaxy luminosity can always be rewritten as:

$$L_G = \langle \alpha_s \rangle N_s \langle M_s v_s^2 \rangle, \quad (24)$$

where the quantities within  $\langle \rangle$  are weighted averages over the whole stellar population. Here  $N_s$  is the number of stars in the galaxy,  $M_s$  their mass and  $v_s^2$  their velocity dispersion. The constant  $\alpha_s$  is different for each galaxy and represents the ratio between the total energy emitted in the form of electromagnetic radiation and the total kinetic energy of the galaxy.

In this context the quantity  $L_0$  can be expressed by the relation:

$$\frac{L_0}{\alpha_s} = M_g = \int_0^t \Psi(t) dt. \quad (25)$$

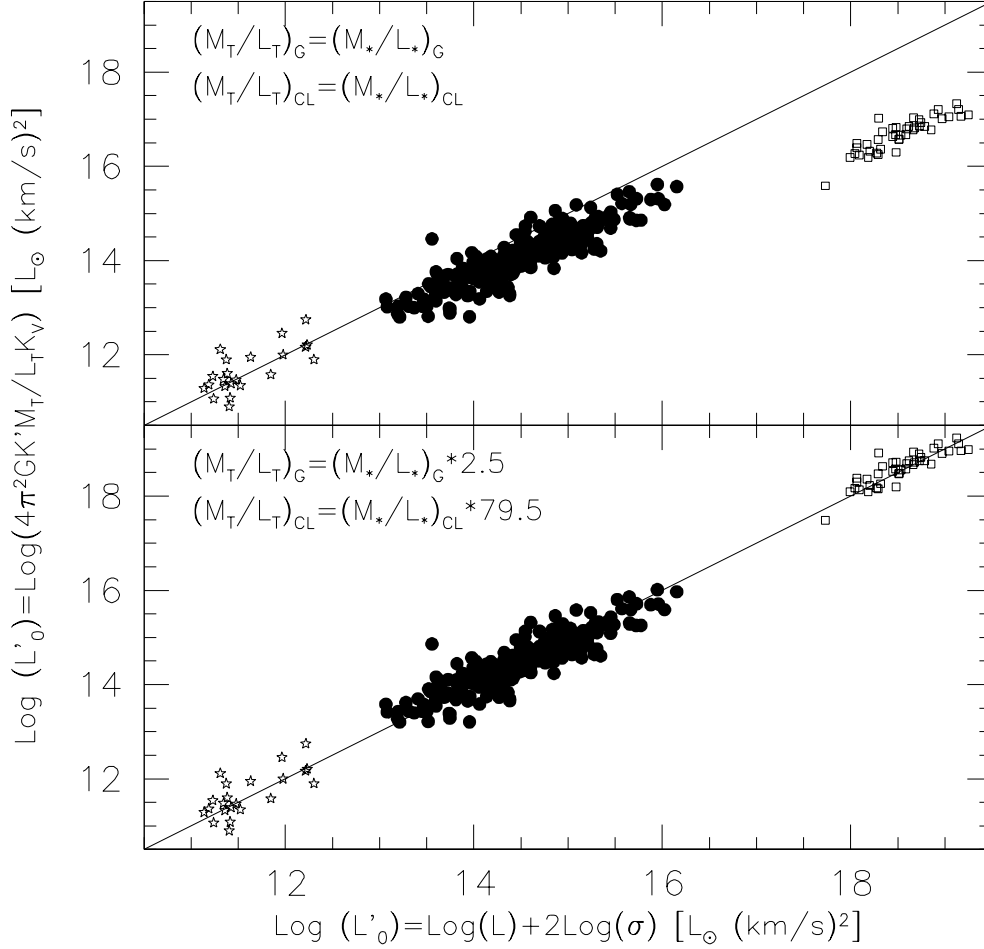


**Figure 10.** Plot of the quantity  $L'_0$  derived from Eq. 22 and from the relation  $L = L'_0 \sigma^{-2}$ .

where we have explicitly written the mass of the galaxy as the integral of its star formation rate and we have highlighted the dependence on time of this parameter.

We can now recast Eqs. (22) and (25) in a different way putting in evidence the star formation rate of a galaxy. From this expression we can argue that at any epoch  $t$  after virialization the SFR could be given by:

$$\Psi(t) = \frac{d}{dt} \left( \frac{4\pi^2 G K'(t) M(t)}{\alpha_s(t) K_V(t)} \frac{1}{L(t) \sigma^4(t)} \right). \quad (26)$$

This relation is an important result because it allows the derivation of the SFR taking into account the projections of the FP in the  $\log(R_e) - \log(\langle I_e \rangle) - \log(\sigma)$  space in a way consistent with observations. In particular we reproduce the ZOE limit in the observed distribution. If we were using the original FJ Eq. (13) with  $\beta = 2$  we would obtain a SFR as a function of time that is proportional to the inverse square of  $\sigma$ . This however would not be consistent with the observed distribution of galaxies in the projections of the FP.

Furthermore the relation of Eq. (26) tells us that at each cosmic epoch the SFR in a galaxy is not free. A galaxy can form stars only at the rate permitted by Eq. (26) along the whole cosmic history after virialization. In other

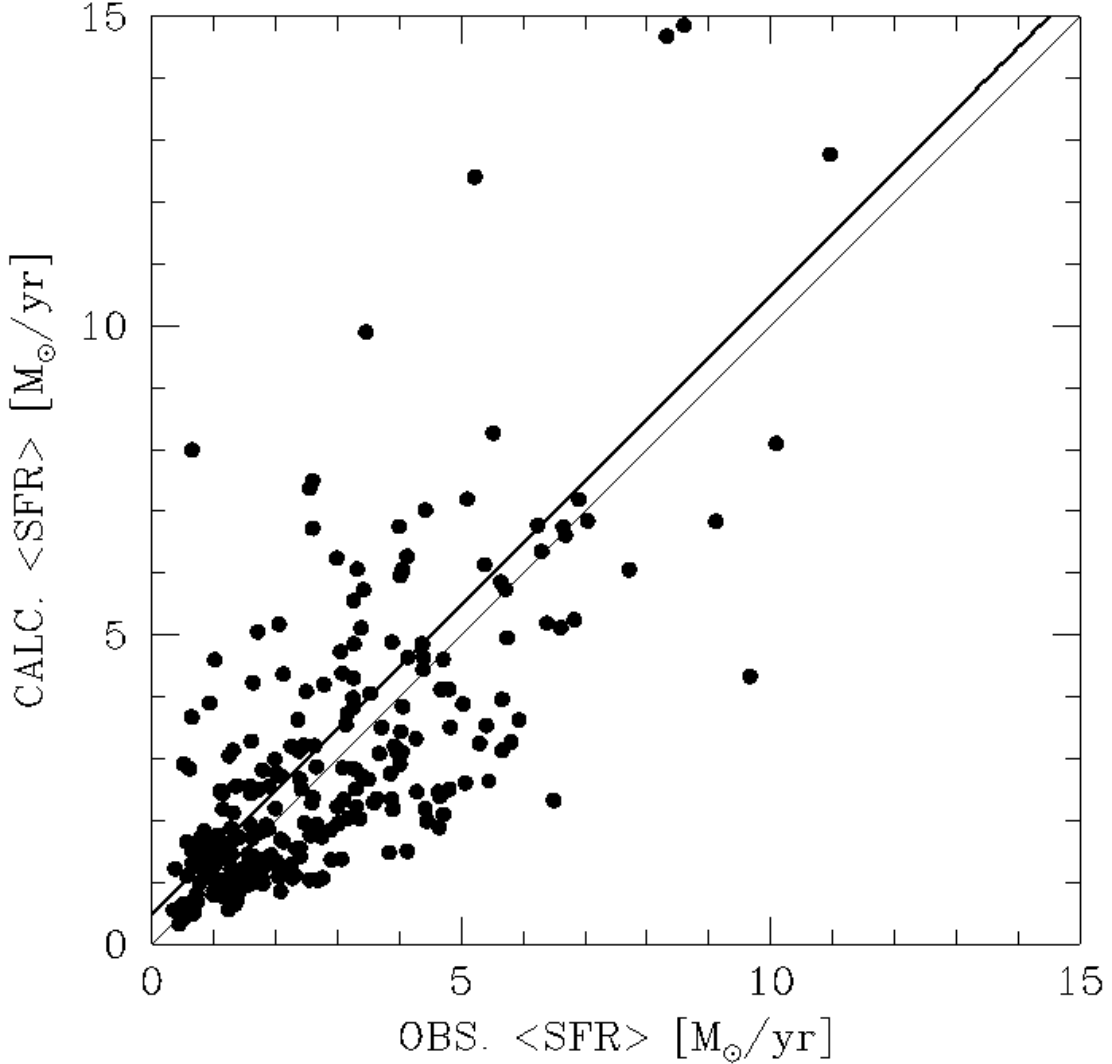


**Figure 11.** Plot of the mean observed SFR measured by Fritz et al. (2007) for the galaxies of the WINGS database using the fitted spectral energy distributions versus the mean  $\langle SFR \rangle$  calculated on the basis of the prediction of Eq. (26) (see text). The thin line is the one-to-one relation, while the thick line is the fitted distribution.

words once the mass and the potential well of a galaxy is given, the star formation can go on according to the galaxy dynamics and to stellar evolution.

If a galaxy does not merge with others and does not experience a significant infall of new gas, its SFR will not be modified considerably continuing its evolution according to Eq. (26). Notably when the velocity dispersion is high the SFR is low. This is observed in today ETGs dominated by an high value of  $\sigma$  and an almost null SFR. Eq. (26) also tells us that when the parameters entering the relation do not change significantly (late stage of evolution) the SFR is naturally around zero, providing a natural explanation for the mass-quenching phenomenon.

Could we test in some way our prediction through observations? Unfortunately testing the validity of Eq. (26) would require a database of masses, luminosities and velocity dispersions at different redshifts, while our WINGS database is made by nearby ETGs only. Considering that at  $t = 0$  the SFR was 0, we can only predict that the mean SFR of today galaxies will be approximately given by:

$$\langle \Psi \rangle = \frac{L_0}{\alpha_s \Delta t} \sim \frac{1}{2} \frac{M_G}{T_G}, \quad (27)$$

where  $\Delta t = T_G$  is the luminosity weighted age of the galaxies.

Fig. 11 shows the mean SFR measured by Fritz et al. (2007) in 4 distinct epochs from the direct fit of the galaxy SEDs versus the mean SFR obtained by Eq. (27). The correlation ( $c.c. = 0.6$  and  $rms \sim 2.8$  but significant at a  $\sim 7\sigma$  confidence level) appears consistent with the theoretical expectation, taking into account the various sources of errors affecting both quantities, even if the sample is biased and the correlation may be driven by few points at high SFR values.

Eq. (26) is probably one key to understand the FP and the star formation history in galaxies. Its actual form depends on the original choice made to formulate the FP problem, but probably behind such relation there is a sort of balance equilibrium among the different forms of energies that are involved in the stellar systems (virial energy, radiation, non baryonic energy, magnetic fields,..). For this reason the next step forward to understand these problems could only come from detailed simulations of galaxy formation and evolution.

## 7. CONCLUSIONS

We have shown that the origin of the FP can be traced back to the validity of two basic physical relations: the virial dynamical equilibrium and the  $L = L'_0\sigma^{-2}$  relation, which is a relation able to explain the existence of the downsizing phenomenon and the nature of the ZOE in the  $I_e - R_e$  plane.

The galaxy luminosity could be correlated in two different ways with the SFR and the velocity dispersion, *i.e.* through the  $L = L'_0\sigma^{-2}$  relation and the  $L = L_0\sigma^2$  relation. The first one is valid for a single galaxy, in the sense that  $L'_0$  is very different for each object, while the second relation is valid for objects of quite different masses (approximately from  $10^9$  to  $10^{12} M_\odot$ ). Both relations have inside them a link with the SFR of galaxies. In the first one the primary role is that played by the SFR/SFH while the velocity dispersion enters as a second less important parameter affecting in some way the SF. On the other hand when the primary role is played by the velocity dispersion we observe that the residuals depend on the SFR (through the  $M/L$  ratio, the effective surface brightness, etc.).

Since, as demonstrated by Zaritsky (2012), a Fundamental Manifold can be constructed for all stellar systems, the easy prediction is that in general the FP and FJ relations are different for each class of stellar system (GCs, dwarf galaxies, late-type galaxies, normal ETGs, cluster of galaxies). The diversity is originated by the different zero-points of the VP and  $L = L'_0\sigma^{-2}$  planes, or in other words by the different SFH and the different coupling between structure, dynamics and stellar populations.

The combination of the virial equilibrium, of the  $L = L'_0\sigma^{-2}$  relation and the validity of the PFJ law for galaxy systems constrain objects of similar characteristics to the same FP, which is the locus of constant  $M/L$  ratio,  $K_V$  and  $SFR$  at each time epoch.

The projection of the intersecting lines connecting the VP and  $L = L'_0\sigma^{-2}$  planes explains the properties observed for ETGs in the  $\log(\langle I_e \rangle) - \log(R_e)$  plane, in particular the existence of the ZOE that in this framework is the natural limit reached by the stellar and dynamical evolution of a stellar system today.

The ZP of the FP provides a natural constraint to the possible SFR activity of a galaxy that at any given epoch could not deviate from the track imposed by the mass and luminosity evolution in a given potential well. Conversely, this relation provides the fine-tuning required to keep galaxies on a tilted FP with a small scatter.

Eq. (26) should be studied now through photometric and dynamical simulations following the details of the mass assembly in stars and their relative luminosities. Naively, we can predict that since the stellar mass is generally increasing, while luminosity and stellar velocity dispersions could vary with the generations of stars, the resulting SFR will probably see various peaks at different redshift epochs depending on the galaxy dynamics.

It will be interesting to see if Eq. (26) will help to quantify the problem of the star formation across the cosmic epochs and constrain in some way the mass quenching phenomenon. First, it will be important to verify if the two principal types of galaxies in the color - magnitude (or stellar mass), color - concentration, and color - morphology diagrams (Strateva et al. 2001; Kauffmann et al. 2003; Brinchmann et al. 2004; Baldry et al. 2004, 2006; Driver et al. 2006; Bamford et al. 2009) can be reproduced. We know that in these plots there are two main regions: the so-called blue cloud (or main sequence), where galaxy mass correlates with the star formation rate, and the red sequence where there is no such correlation and galaxies are passive. The origin of this bi-modality is commonly attributed to the bulge and disk structure of galaxies. In general disks are bluer in color than bulges (e.g., Peletier & Balcells 1996) and galaxies with lower stellar mass and lower Sersic index tend to be bluer (and hence have higher sSFRs) than higher stellar mass and higher Sersic index systems (Baldry et al. 2004; Driver et al. 2006; Baldry et al. 2006; Bamford et al. 2009). Similar trends are observed for luminosity and stellar light concentration (Strateva et al. 2001; Driver et al. 2006). This idea fits with the found dependence of the SFR on the Sersic index and velocity dispersion found here.

Unfortunately all such relationships are complicated by the effects of the environment, so that disentangling the various effects on the star formation efficiency is quite difficult.

## APPENDIX

### A. A POSSIBLE ORIGIN FOR THE FJ RELATION

We try to demonstrate here that the FJ relation could be seen as a sort of translation of the Black Body Stefan-Boltzmann law valid for individual stars to the case of a galaxy made by an assembly of stars in which the temperature is replaced by the velocity dispersion. From this analysis it will appear again the link connecting  $L_0$  and  $L'_0$  with the SFR of galaxies.

It goes without saying that there is not an immediate straight correlation between the physical situations in stars and galaxies; however, we will convincingly see that such analogy is possible and also argue that dynamics (via the velocity dispersion) and stellar populations in a galaxy (via the light emitted by stars) are each other intimately related. To demonstrate that this is possible we proceed as follow.

#### A.1. The case of single stars

A star of mass  $M_s$ , radius  $R_s$ , luminosity  $L_s$ , and effective temperature  $T_{s,e}$  is an assembly of  $N$  heavy particles (nuclei, ions, and atoms, whereas electrons can be neglected) in thermal motion with mean temperature  $\langle T \rangle$  and in virial equilibrium, i.e. satisfying the condition:

$$M_s v_s^2 \equiv \left| \frac{GM_s^2}{R_s} \right| \equiv E_V \quad (\text{A1})$$

where  $v_s$  is the mean particle velocity in a gram of matter,  $M_s = N \langle m_p \rangle$  with  $N$  is the number of heavy particles and  $m_p$  their mean mass, and finally  $E_V$  stands for the "virial energy".

Consider first the total bolometric luminosity of a star (i.e. the total energy emitted per second by the surface). This is usually derived from the Stefan-Boltzmann law, since stars are in good approximation Black Body systems.

In a star we can measure the luminosity  $L_s$ , the effective temperature  $T_{es}$ , and the radius  $R_s$  which are related by the well known Black Body law ( $L = 4\pi R^2 \sigma_{SB} T^4$ ), where  $\sigma_{SB}$  is the Stefan-Boltzmann constant. The suffix  $SB$  is to distinguish it from the velocity dispersion of stars in a galaxy, usually indicated with the same symbol. When misunderstanding is obviously avoided, the suffix is dropped.

It is worth recalling here that the luminosity can be derived from the energy content of the Black Body according to:

$$U_{bb}(T) = \frac{8\pi\Omega}{h^3 c^3} (kT)^4 \frac{\pi^4}{15} \quad (\text{A2})$$

where  $\Omega$  is the total volume and  $U_{bb}(T)$  the total energy of the Black Body. From this we obtain the luminosity of the star

$$L_s = \frac{U_{bb}(T)}{\Omega} 4\pi R_s^2 c = \frac{3U_{bb}(T)c}{R_s}. \quad (\text{A3})$$

At this point we verify that the gravitational energy, the mean kinetic energy of the particles, and the Black Body energy content of the whole star with mean temperature  $\langle T \rangle$  are comparable to each other. Taking the Sun as a typical star, for which we assume  $R_s = 6.94 \cdot 10^{10}$  cm,  $M_s = 1.99 \cdot 10^{33}$  g, mean internal temperature  $\langle T \rangle \simeq 5 \cdot 10^6$  K, and central value  $T \simeq 10^7$ ,<sup>3</sup> we obtain:

i) the mean density of kinetic energy of the  $N$  particles in the star is

$$\langle E_k \rangle = \frac{1}{\Omega} \sum_i^N \frac{m_p v_p^2}{2} = \frac{3}{2} n k T \simeq 3.47 \times 10^{15} \text{ erg/cm}^3 \quad (\text{A4})$$

<sup>3</sup> The elementary theory of stellar evolution by combining the equations for hydrostatic equilibrium, mass conservation and physical state of the plasma, e.g.  $P = \frac{k}{\mu m_H} \rho T$ , provides a simple relation for the mean temperature inside a star

$$\bar{T} \geq 4.58 \times 10^6 \mu \frac{M}{M_\odot} \frac{R_\odot}{R} \text{ K}$$

where  $M$  and  $R$  are the total mass and radius of the star and  $\mu$  the mean molecular weight of the gas. For a solar like star  $\mu \simeq 1$ , so that  $\bar{T} \simeq 5 \cdot 10^6$ . The central temperature is higher than this and close to  $10^7$ .

where  $m_p$  and  $v_p$  are the mass and velocity of each particle and  $n = N/\Omega$  is the number density of particles.

ii) the mean density of gravitational energy is

$$\langle E_g \rangle = \frac{3GM_s^2}{4\pi R_s^4} \simeq 2.72 \times 10^{15} \text{ erg/cm}^3 \quad (\text{A5})$$

iii) the mean energy density of the photons is

$$\langle U_{bb}(T) \rangle = \frac{8\pi^5}{15h^3c^3}(KT)^4 \simeq 1.15 \times 10^{15} \text{ erg/cm}^3 \quad (\text{A6})$$

for a mean temperature of  $10^7$  K. Within the numerical approximation the three energies are of the same order. Strictly speaking one should have  $\langle E_g \rangle \simeq \langle E_k \rangle + \langle U_{bb} \rangle$ . Within the approximation our estimates fulfill this constraint. Analogous estimates can be made for other types of star with similar conclusions. In other words, there seems to be a relationship between the gravitational energy density and the sum of the electromagnetic and kinetic energy densities. Finally, using the virial condition we can also estimate the mean velocities of the particles in a star (the Sun in this example) which are about  $v_s \simeq 200$  km/s, depending on the exact value adopted for the temperature.

Given these premises, the luminosity of a star can be derived from

$$L_s = \left| \frac{dE_i}{dt} \right|, \quad (\text{A7})$$

where  $E_i$  is the total internal energy (sum of the nuclear and gravo-thermal contributions). We may generalize the above relation by supposing that the luminosity can be expressed as:

$$L_s = \alpha_s E_V \equiv \alpha_s M_s \langle v_p \rangle^2 \equiv \alpha_s \langle U_{bb} \rangle \frac{4}{3} \pi R_s^3 \quad (\text{A8})$$

where  $\alpha_s$  is a suitable proportionality factor with the dimension of an inverse of time. In other words we link the luminosity  $L_s$  to the internal properties of the star, in particular to the mean velocity of the constituent heavy particles.

However the same luminosity can be expressed by means of the surface Black Body with temperature equal to the effective temperature  $T_e$  of the star (a few thousands degrees, about  $5.78 \times 10^3$  K for the Sun and  $3 \times 10^3$  for a RGB star).

$$L = \langle U'_{bb} \rangle 4\pi c R_s^2 \quad (\text{A9})$$

where  $U'_{bb}$  is the energy of the black body at the surface temperature. This implies that the ratio of the external to the internal Black Body energies is  $U'_{bb} \simeq 10^{-13} U_{bb}$ . The size of the proportionality coefficient can be understood as due to the  $T^4$  dependence of the Black Body energy density and the natural variation of the temperature from the surface to the inner regions of a star. The typical temperature gradient of a Sun like star is  $\|\Delta T/\Delta R\| \simeq 10^{-4} \text{ K cm}^{-1}$ , where  $\Delta T = T - T' \simeq T$  and  $\|\Delta R\| = \|R - R'\| \simeq R'$  if R and T refer to a inner region (close to the center) and  $R'$  and  $T'$  to the surface. Therefore  $T'/T \simeq 10^{-4}$ .<sup>4</sup>

It follows from all this that  $\alpha_s \simeq 10^{-14} c/R_s$ . Inserting the value for the light velocity and the radius of a typical star (like the Sun) one obtains  $\alpha_s \simeq 10^{-14} \text{ s}^{-1}$ .

The factor  $c/R_s$  secures that the energy density is translated to energy lost per unit time (a power). What we have done so far is a simple rephrasing of the classical expression for the luminosity. The reason for writing the star luminosity in this curious way will appear clear as soon as we move to galaxies, *i.e.* to systems hosting billion of stars.

The whole discussion above has been checked against stars like the Sun, so that one expect that changing type of stars the value of  $\alpha_s$  should change. This is shown in Fig. 12. As expected  $\alpha_s$  spans a wide range passing from dwarfs to massive stars, but this will not affect our final conclusions.

<sup>4</sup> The values assumed for the central and surface temperature of the Sun amply justify a ratio  $T'/T \simeq 0.0001$  or lower and a proportionality factor  $10^{-13}$  in the relationship between the energy densities  $U_{bb}$  and  $U'_{bb}$ .

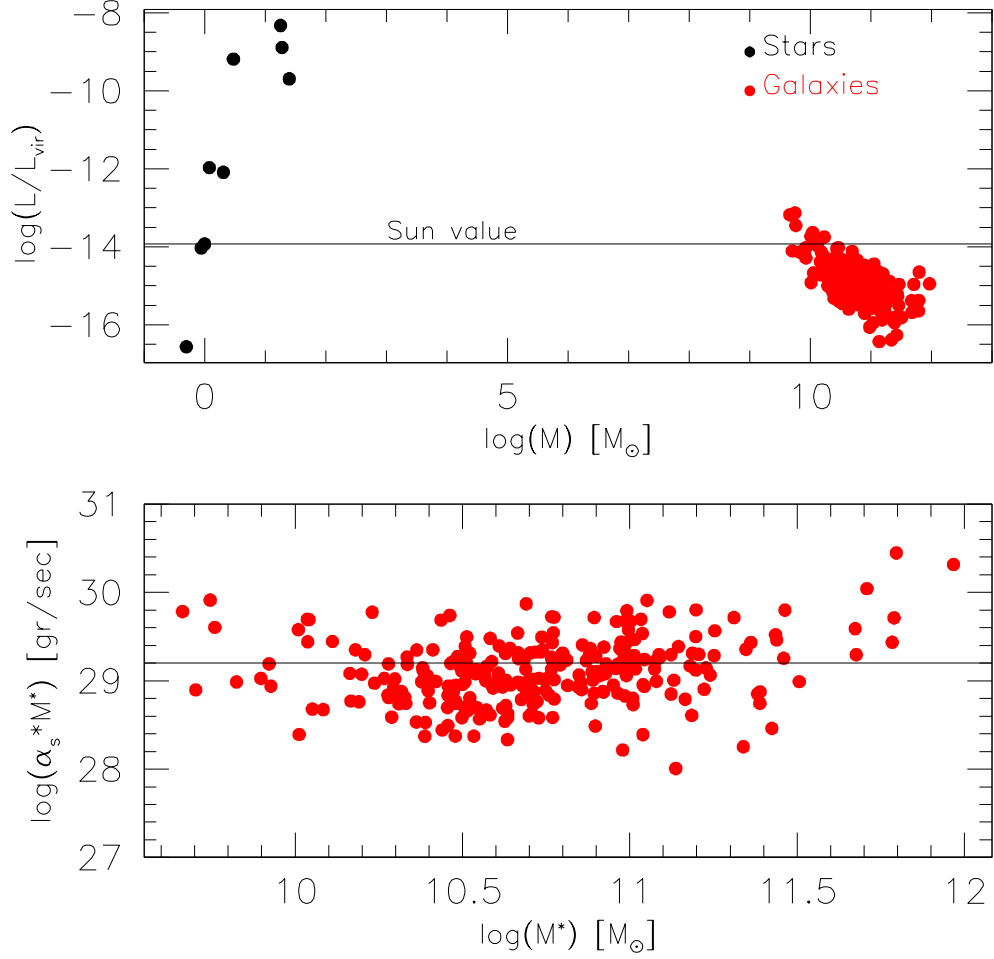


**Figure 12.** Upper panel: Plot of  $\alpha_s$  for the stars and its analog for the galaxies  $\alpha_G$  (see the text for the definition) as a function the mass of the virialized system (star or galaxy as appropriate). Note the large range of values spanned by  $\alpha_s$  at varying the mass of the star from a dwarf to a massive object. Finally note that the values  $\alpha_G$  for the galaxies fall in range typical of the low mass (old) stars. Lower panel: plot of  $L_0 = \alpha_s * M_G$  (using  $M^*$  instead of  $M_G$ ) versus the galaxy masses. The solid line gives the value observed for  $L_0$  in the FJ relation.

### A.2. The case of galaxies

We extend now the above consideration and formalism to the case of a galaxy with mass  $M_G$  and radius  $R_G$ , a large assembly of stars each of which shining with the luminosity  $L_{s,i}$ . In brief, the luminosity of the galaxy is the sum of the luminosity of the all the stars inside; the luminosity of each star can be expressed as proportional to the total kinetic energy of gas particles. Therefore we may write

$$L_G = \sum_{i=1}^{N_s} \alpha_{s,i} M_{s,i} v_{s,i}^2, \quad (\text{A10})$$

where  $N_s$  is the total number of stars within the galaxy, and  $\alpha_{s,i}$ ,  $M_{s,i}$ ,  $v_{s,i}$ , and  $R_{s,i}$  are the basic quantities characterizing each star. In analogy with eq. (A.1), the galaxy luminosity can be rewritten as:

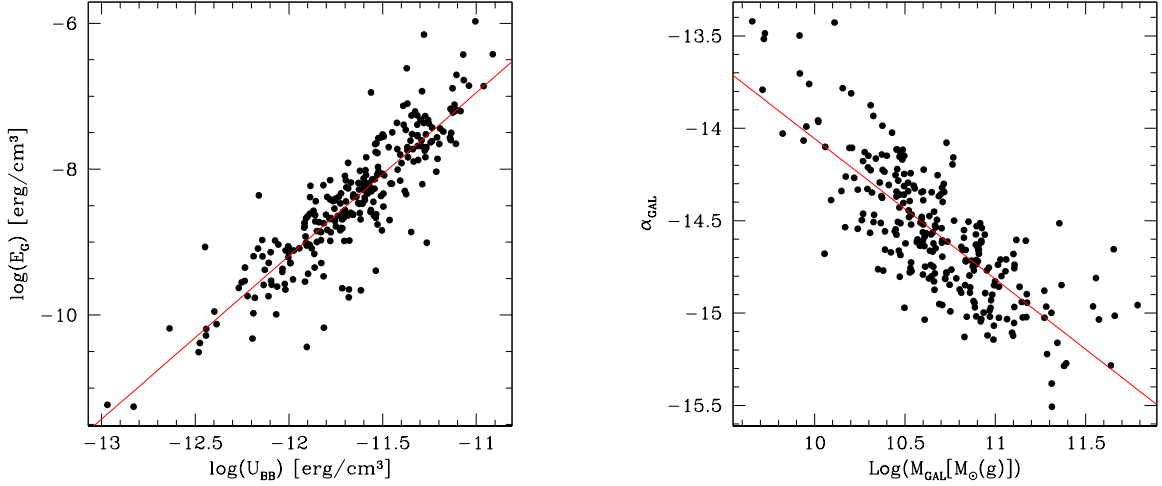


**Figure 13.** Left panel: The mean density of the gravitational energy versus the mean density of the BB energy for a sample of early type galaxies. Right Panel: the quantity  $\alpha_G$  as function of the stellar galaxy mass in solar units for the object of the same sample.

$$L_G = \langle \alpha_s \rangle N_s \langle M_s v_s^2 \rangle, \quad (\text{A11})$$

where the quantities within  $\langle \rangle$  are weighted averages over the whole stellar population. Note that for galaxies of the same "size" (mass and radius) these values will be very similar.

Now, thanks to the homologous nature of the gravitational collapse at all scales, it is possible to note that the quantity  $\langle v_s \rangle$ , i.e. the mean velocity of particles inside a star, turns out to be comparable to the velocity dispersion of stars within a galaxy, customarily named  $\sigma$  (in km/sec). It is then possible to write:

$$L = L_0 \sigma^2, \quad (\text{A12})$$

where

$$L_0 = \langle \alpha_s \rangle N_s \langle M_s \rangle \equiv \langle \alpha_s \rangle M_G. \quad (\text{A13})$$

It can be shown that even for a galaxy there is a relationship (by chance?) between the total gravitational energy, the total kinetic energy of the stars, and total radiative energy emitted by stars so that the relation (A13) can be replaced by

$$L_0 = \langle \alpha_G \rangle M_G \equiv \frac{c}{R_G} M_G \quad (\text{A14})$$

where  $\alpha_G$  refers to the galaxy as a whole. Like in the case of stars,  $\langle \alpha_G \rangle$  has the dimension of an inverse of time.

To demonstrate the validity of Eq. (A14) we consider a generic mean stellar content of  $N_s \simeq 10^{12}$  objects for simplicity taken like to the Sun ( $M_{\odot} = 2 \times 10^{33}$  g and radius  $R_{\odot} = 6.94 \times 10^{10}$  cm, surface temperature  $T_s \simeq 5780$  K), total mass  $M_G = 10^{12} M_{\odot}$ , total radius  $R_G \simeq 100$  kpc. In this example we ignore the contribution to the mass given by Dark Matter (DM). According to the current understanding of the presence of DM in galaxies, the ratios of the dark to baryonic matter (BM) both in mass and radii of the spatial distributions (supposed to spherical)  $M_{DM} \simeq \beta \times M_{BM}$  and  $R_{DM} = \beta \times R_{BM}$ . This means that within the volume occupied by the BM there is about  $1/\beta^2 \times M_{DM}$  (Bertin, Saglia, & Stiavelli 1992; Saglia, Bertin, & Stiavelli 1992; Bertin et al. 2002). For current estimates of  $\beta \simeq 6$  DM can be neglected in the internal regions of a galaxy where stars are located.

The energy density of the photons emitted by all the stars in the galaxy evaluated at any arbitrary point inside the galaxy is given by

$$U_{bb,G} = \int_0^{R_G} U'_{bb,s} \frac{N_s}{\Omega_G} 4\pi r^2 dr \frac{R_s^2}{r^2} \quad (\text{A15})$$

where  $U'_{bb,s}$  refers to the Black Body at the temperature of the stellar sources<sup>5</sup>,  $\Omega_G$  is the volume of the whole galaxy, and the factor  $U'_{bb,s} \times N_s/\Omega_G$  the mean Black Body radiation inside the galaxy. Although the integrand of Eq. (A15) is not strictly correct to evaluate the variation of the Black Body energy as a function of the galacto-centric distance, it is adequate to our purposes. The quantity  $U'_{bb,s}$  is given by

$$U'_{bb,s} = \frac{8\pi}{h^3 c^3} \frac{\pi^4}{15} (kT)^4 \simeq 8.02 \text{ erg cm}^{-3} \quad (\text{A16})$$

so that for  $U_{bb,G}$  of eq. (A15) we estimate

$$U_{bb,G} \simeq 1.29 \times 10^{-12} \text{ erg cm}^{-3} \quad (\text{A17})$$

where we assumed  $N_s \simeq 10^{12}$  stars,  $R_s \simeq 6.94 \times 10^{10}$  cm (roughly the solar radius),  $\Omega_G \simeq 1.13 \times 10^{71}$  cm<sup>3</sup> for a galactic radius of about 100 kpc.

The mean density of kinetic energy of the stars turns out to be of the order of  $3.52 \times 10^{-12}$  erg cm<sup>-3</sup> for a mean velocity dispersion of about 200 km s<sup>-1</sup>.

The mean gravitational energy density for the galaxy (limited to the volume occupied by the BM) is

$$E_{g,G} = G \frac{M_G^2}{R_G^4} \frac{3}{4\pi} \simeq 7.79 \times 10^{-12} \text{ erg cm}^{-3} \quad (\text{A18})$$

The gravitational energy is surely underestimated because we have neglected the presence of Dark Matter.

Therefore, also in this case there is an approximate relationship between the gravitational and the sum of electromagnetic and kinetic energy densities.

We can then write the equation:

$$L_G = \alpha_G M_G \sigma^2 = \alpha_G < U_G > R_G^3. \quad (\text{A19})$$

Thanks to the assumption of uniform distribution of stars and stellar types most contributing to the light in our model galaxy, also the distribution of the photon energy inside is uniform and always equal to the that of many black bodies of similar temperature. Furthermore, owing to the very large number of stars in a galaxy the light emitted by a certain region, e.g. within the effective radius, can be assimilated to that of black body of certain mean temperature and very large surface. Therefore we may write

$$L_G = < U_{bb,G} > 4\pi c R_G^2 \quad (\text{A20})$$

so that for solar like stars  $\alpha_G \simeq c/R_G \simeq 10^{-13} \text{ s}^{-1} \simeq \alpha_s$ . It is worth emphasizing here that  $\alpha_G$  is nearly identical to  $\alpha_s$ .

In conclusion the classical Faber-Jackson relationship  $L = L_0 \sigma^2$  can be understood as a sort of translation of Stefan-Boltzmann law for BBs to the case of galaxies that can be viewed as the sum of many BBs.

Fig. 12 shows the range of values for the parameter  $\alpha_G$  of galaxies and compares them with those for stars. Note that low mass galaxies have in general higher values of  $\alpha$  (closer to the values for intermediate mass stars), whereas the big galaxies are preferentially populated by low mass stars. What matters here is that for every galaxy it exists a combination of  $L_0$  ( $\sim \alpha_s M_G$ ) and  $\sigma$  able to reproduce the total galaxy luminosity. The lower panel of Fig. 12 shows that  $L_0 = \alpha_s * M_G$  is approximately constant for wide range of galaxy masses.

We have calculated  $U_{bb,G}$  and  $E_g$  for a small sample of early type galaxies (Moretti et al. 2014) for which all the basic data were available and estimated the parameter  $\alpha_G$  for all of them. The results are shown in the two panels of Fig. 13.

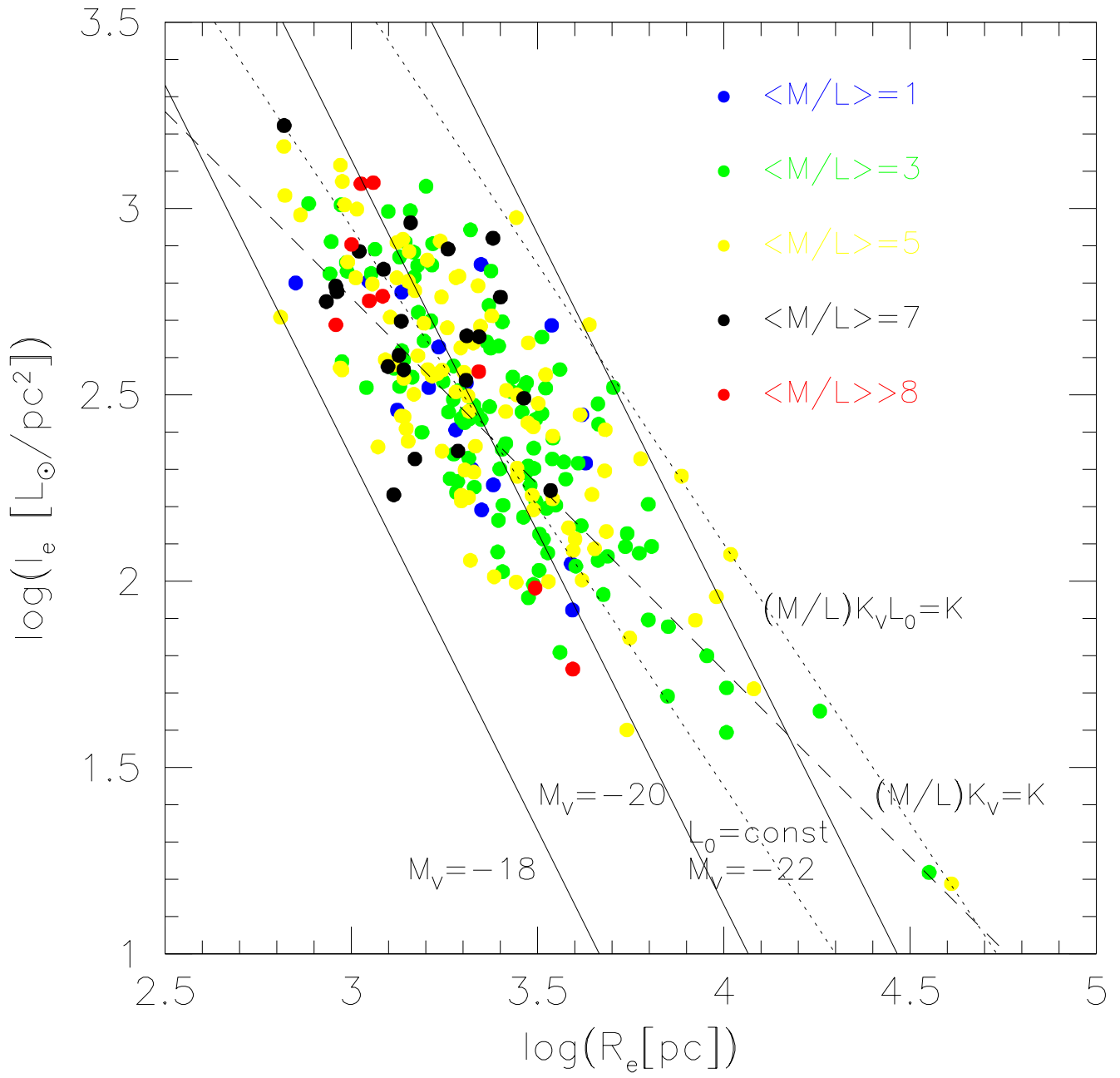
One might argue whether this is true also for spiral galaxies. We believe that the origin of the Tully-Fisher relation for late-type systems can be likely reported to the same context. Here the mean characteristic velocity of the stellar system is no longer the velocity dispersion, but the circular rotation. For more complex systems, where rotation and velocity dispersion are significant, a combination of the two is required to characterize the total kinetic energy. The issue, however, is left to a future investigation.

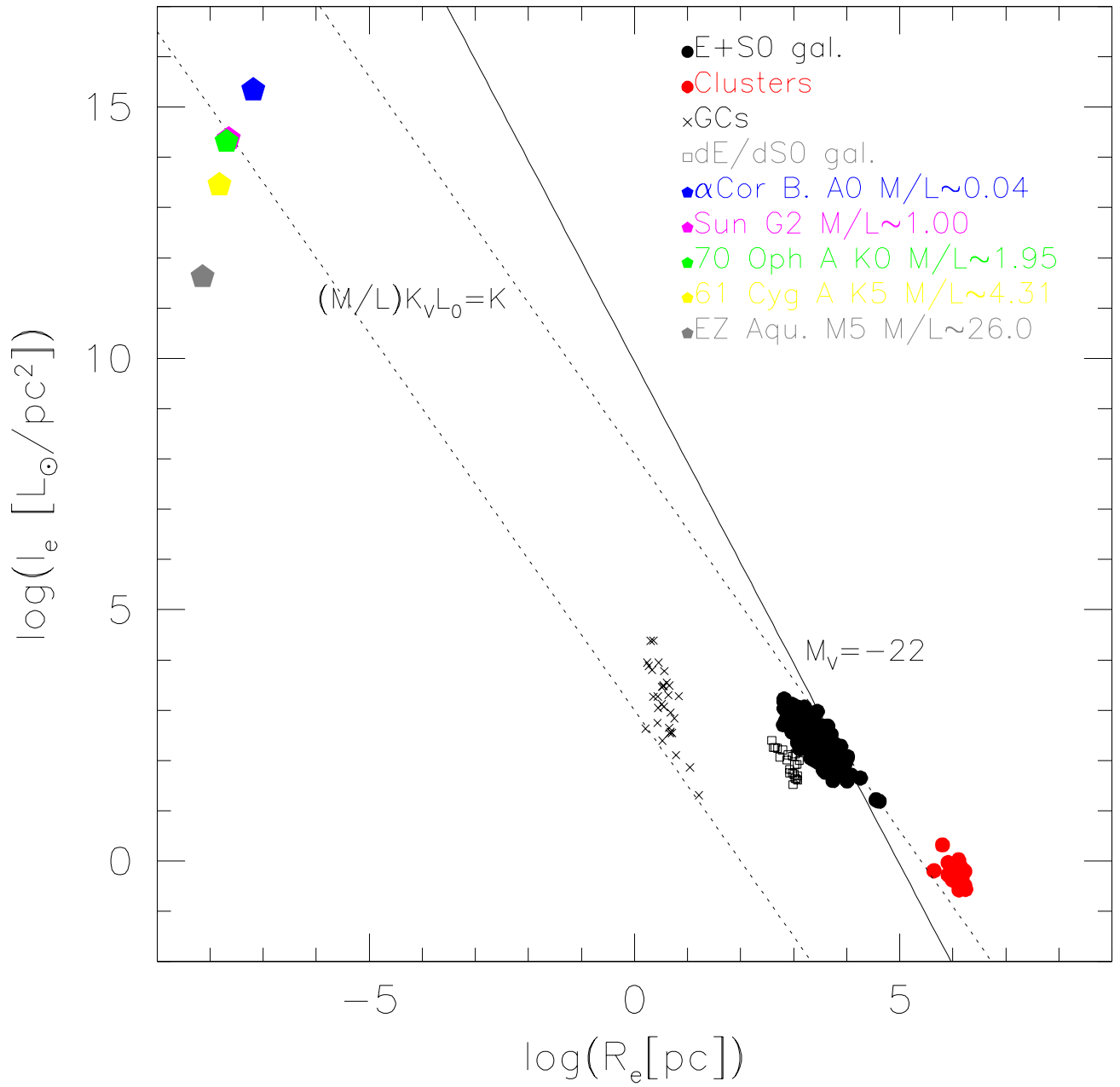
## REFERENCES

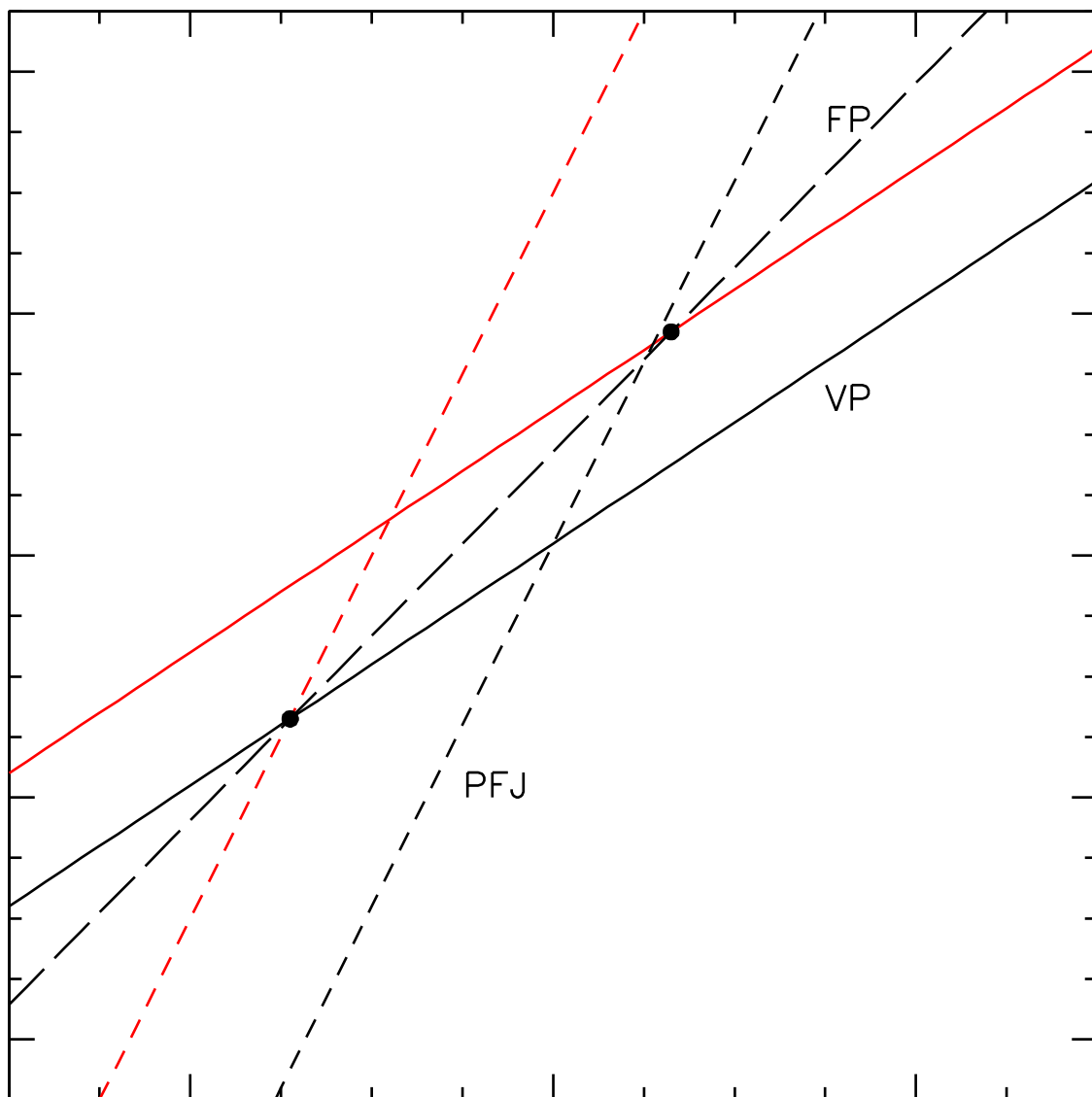
<sup>5</sup> In relation to this, we remind the reader that in most galaxies nearby the detected light is due to stars from the main sequence turnoff (or slightly fainter than) to the tip of the RGB. In sufficiently old galaxies the corresponding mass range is rather small. In other words, the stellar population responsible for the observed light can be reduced to a single population of a certain age and mean chemical composition.

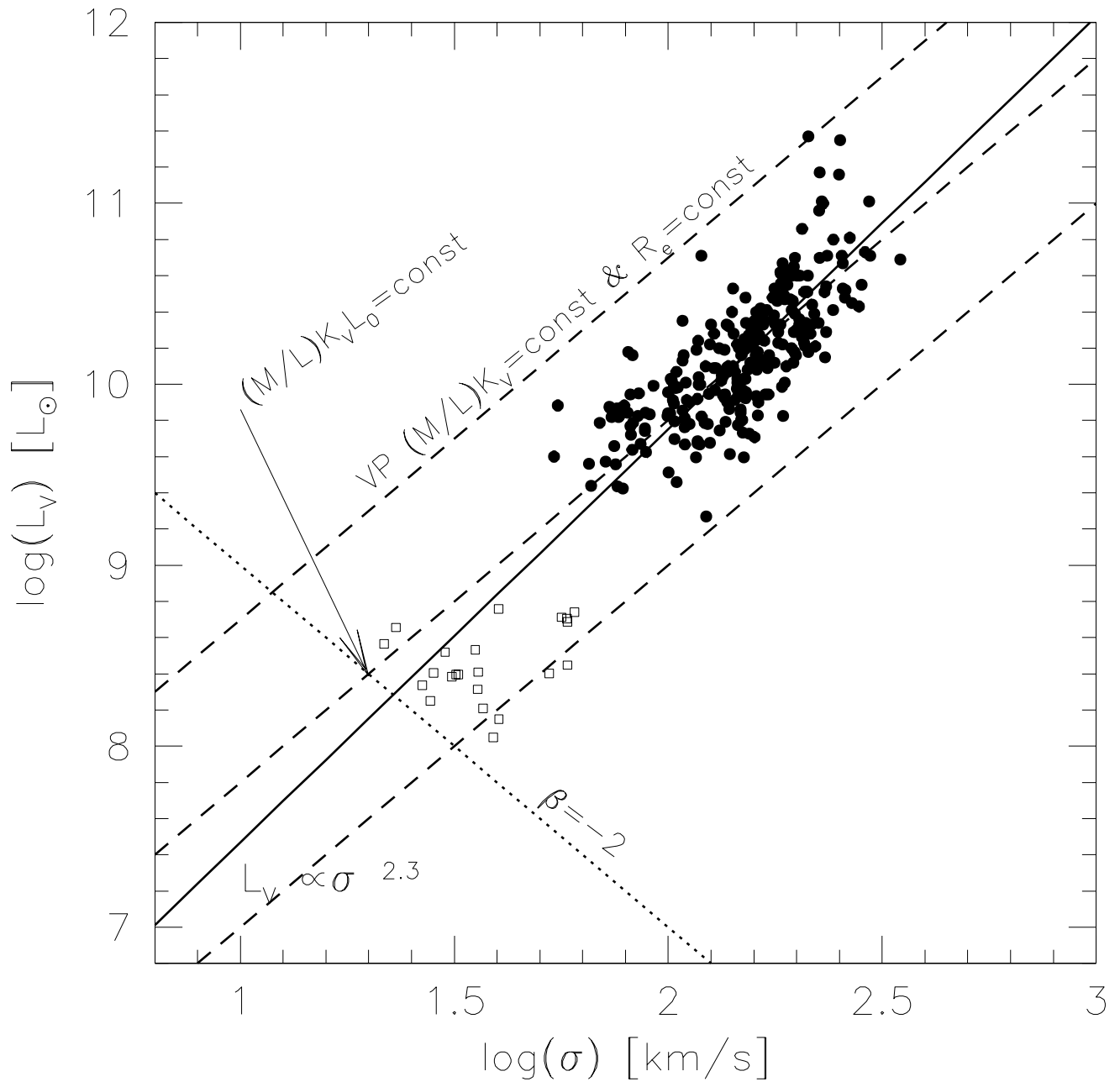
- Baldry I. K., Glazebrook K., Brinkmann J., Ivezić Z., Lupton R. H., Nichol R. C., Szalay A. S. 2004, *ApJ*, 600, 681
- Baldry I. K., Balogh M. L., Bower R. G., Glazebrook K., Nichol R. C., Bamford S. P., Budavari T. 2006, *MNRAS*, 373, 469
- Bamford S. P. et al. 2009, *MNRAS*, 393, 1324
- Bender R., Burstein D., Faber S.M. 1992, *ApJ*, 399, 462
- Bertin G., Saglia R. P., Stiavelli M. 1992, *ApJ*, 384, 423
- Bertin G., Ciotti L., Del Principe M. 2002, *MNRAS*, 386, 149
- Borriello A., Salucci P., Danese L. 2001, *MNRAS*, 341, 1109
- Bolton A.S., Treu T., Koopmans L.V. E., et al. 2008, *ApJ*, 684, 248
- Brinchmann J., Charlot S., White S. D. M., Tremonti C., Kauffmann G., et al. 2004, *MNRAS*, 351, 1151
- Burkert A. 1993, *A&A*, 278, 23
- Burstein D., Bender, R., Faber, S.M., Nolthenius, R. 1997, *AJ*, 114, 1365
- Busarello G., Capaccioli M., Longo G., Puddu E. 1997, In: The Second Stromlo Symposium “The nature of Elliptical Galaxies”, ASP Conference Series, 166, 184
- Caon N., Capaccioli M., D’Onofrio M. 1993, *MNRAS*, 265, 1013
- Capaccioli M. 1987, In: Structure and dynamics of elliptical galaxies, ed. P.T. de Zeeuw (Reidel, Dordrecht), p. 47
- Capaccioli M. 1989, In: The world of galaxies, ed. H.G. Corwin & L. Bottinelli (Springer-Verlag, Berlin), p. 208
- Cappellari M., Bacon R., Bureau M., et al. 2006, *MNRAS*, 366, 1126
- Cappellari M., Emsellem E., Bacon R., et al. 2007, *MNRAS*, 379, 418
- Cappellari M., McDermid R.M., Alatalo K., et al. 2012, *Nature*, 484, 485
- Cappellari M., McDermid R.M., Alatalo K., et al. 2012, *MNRAS*, 432, 1862
- Chiosi C., Bressan A., Portinari L., Tantalo R. 1998, *A&A*, 339, 355
- Chiosi C., Carraro G. 2002, *MNRAS*, 335, 335
- Ciotti L., Lanzoni B., Renzini A. 1996, *MNRAS*, 282, 1
- de Carvalho, R.R., da Costa L.N. 1988, *ApJS*, 68, 173
- Dekel A., Cox T.J. 2006, *MNRAS*, 370, 1445
- Desmond H., Wechsler R.H. 2016, 2016arXiv160404670D
- Djorgovski S., Davis M. 1987, *ApJ*, 313, 59
- Djorgovski S., De Carvalho R., Han S.M. 1988, *ASPC*, 4, 329
- D’Onofrio M., Fasano G., Moretti A., Marziani P., et al. 2013, *MNRAS*, 435, 45
- Dressler A., Lynden-Bell D., Burstein D., Davies R.L., Faber S.M., Terlevich R.J., Wegner G. 1987, *ApJ*, 313, 42
- Driver S. P. et al. 2006, *MNRAS*, 368, 414
- Faber S.M., Dressler A., Davies R., Burstein D., Lynden-Bell D. 1987, In: Nearly normal galaxies: From the Planck time to the present; Proceedings of the Eighth Santa Cruz Summer Workshop in Astronomy and Astrophysics, Santa Cruz, CA, July 21-Aug. 1, 1986 (A88-18401 05-90). New York, Springer-Verlag, 1987, p. 175-183
- Faber S.M., Jackson R.E. 1976, *ApJ*, 204, 668
- Forbes D.A., Ponman T.J., Brown R.J.N. 1998, *ApJ*, 508, L43
- Fritz J., Poggianti B. M., Bettoni D., et al. 2007, *A&A*, 470, 137
- Gargiulo A. 2009, *MNRAS*, 397, 75
- Gerhard O., Kronawitter A., Saglia R.P., Bender R. 2001, *AJ*, 121, 1936
- Graham A., Colless M. 1997, *MNRAS*, 287, 221
- Graves G.J., Faber S.M., Schiavon R.P. 2009, *ApJ*, 698, 1590
- Hjorth J., Madsen J. 1995, *ApJ*, 445, 55
- Hopkins Ph.F., Cox T.J., Hernquist L. 2008, *ApJ*, 689, 17
- Kauffmann G. et al. 2003, *MNRAS*, 346, 1055
- Kormendy J. 1977, *ApJ*, 218, 333
- La Barbera F., Busarello G., Capaccioli M. 2000, *A&A*, 362, 851
- La Barbera F., de Carvalho R. R., de La Rosa I. G., Lopes P. A. A. 2010, *MNRAS*, 408, 1335
- Magoulas C., et al. 2012, *MNRAS*, 427, 245
- Michard R. 1985, *A&AS*, 59, 205
- Moretti A., et al. 2014, *A&A*, 564, 138
- Nipoti C., Londrillo P, Ciotti L. 2006, *MNRAS*, 370, 681
- Oñorbe J., Domínguez-Tenreiro R., Sáiz A., Serna A., Artal H. 2005, *ApJ*, 632, L57
- Pasquato M., Bertin G. 2008, *A&A*, 489, 1079
- Pahre M.A., De Carvalho R.R., Djorgovski S.G. 1998, *AJ*, 116, 1606
- Peletier R. F., Balcells M. 1996, *AJ*, 111, 2238
- Prugniel Ph., Simien F. 1997, *A&A*, 321, 111
- Renzini A., Ciotti L. 1993, *ApJ*, 416, L49
- Robertson B., Cox T.J., Hernquist L., et al. 2006, *ApJ*, 641, 21
- Saglia R. P., Bertin G., Stiavelli M., 1992, *ApJ*, 384, 433
- Schombert J.M. 1986, *ApJS*, 60, 603
- Scoddeggio M., Gavazzi G., Belsole E., Pierini D., Boselli A. 1998, *MNRAS*, 301, 1001
- Secco L. 2001, *New Astr.* 6, 339
- Secco L, Bindoni D. 2009, *New Astr.* 14, 567
- Strateva I., et al. 2001, *AJ*, 122, 1861
- Terlevich A.I., Forbes D.A. 2002, *MNRAS*, 330, 547

- Tortora C., Napolitano N. R., Romanowsky A. J.,  
Capaccioli M., Covone G. 2009, MNRAS, 396, 1132
- Treu T., Ellis R.K., Liao T.X., van Dokkum P.G. 2005,  
ApJ, 622, L5
- Trujillo I., Burkert A., Bell E.F. 2004, ApJ, 127, 1917
- Tully B.R., Fisher J.R. 1977, A&A, 54, 661
- Young C.K. & Currie M.J. 1994, MNRAS, 268, 11
- Zaritsky D. 2012, ISRN Astronomy and Astrophysics, vol.  
2012, id. 189625









Subscription and author costs

